Prof. Daniel Balzani
Ruhr Universität Bochum
Chair of Continuum Mechanics

Luigi E. Perotti, PhD
University of Central Florida
Computational Biomechanics Lab

Computing Meets Cardiology: Making Heart Simulations Fast and Accurate

Dennis Ogiermann

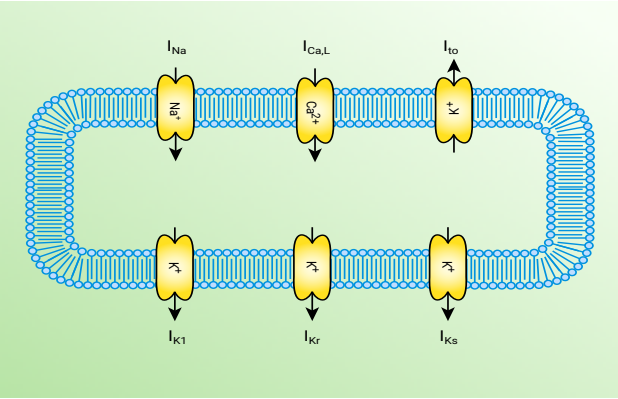

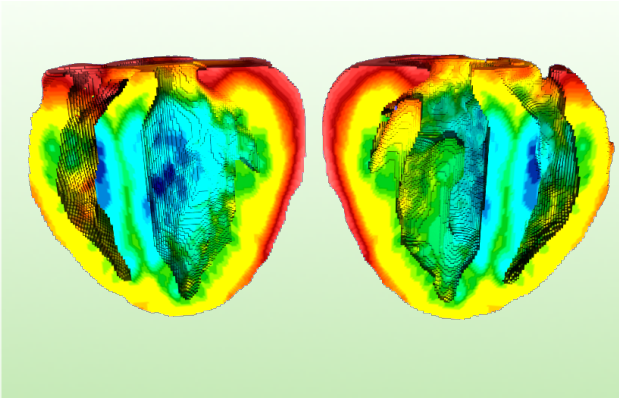

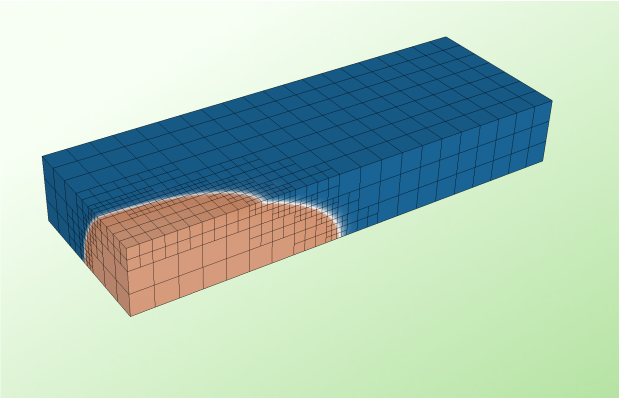

- Cardiac Anatomy and Physiology 101
- Cardiac Electrophysiology
- Forward Problem of Electrocardiology
- Bidirectionally Coupled Electromechanics

Motivation

- Cardiovascular diseases are a leading cause of death worldwide WHO [2017]
- Heart diseases are a huge socioeconomic burden AHA [2017]
- Computational models to gain insights into cardiac function

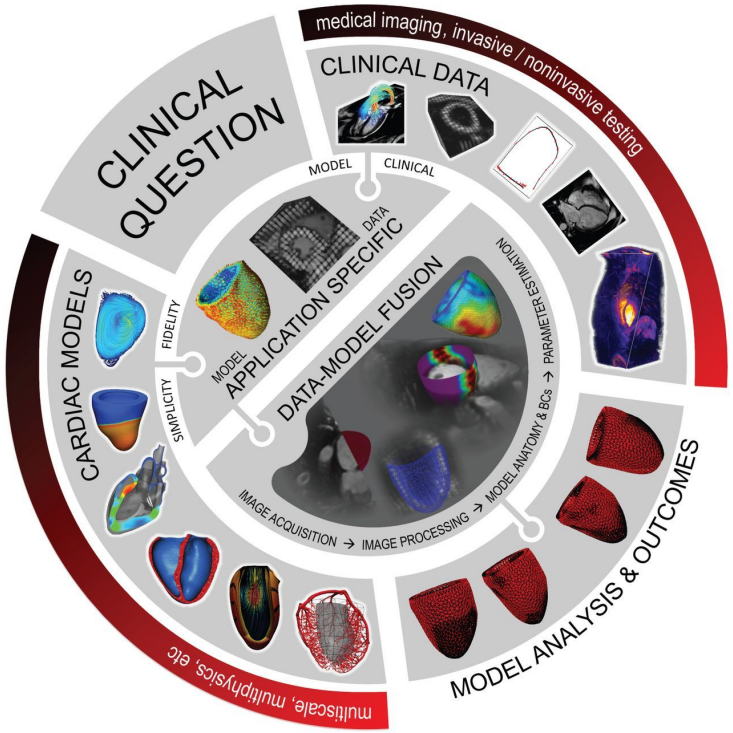

Chabiniok et al. [2016]

Luigi Perotti

Challenges

- Multiple temporal and spatial scales
- Multiphysics
- Uncertainties due to stochasticity

Goal

Flexible computational environment to explore cardiac function

Overview

Basic Cardiac Anatomy and Function

Cardiac Electrophysiology

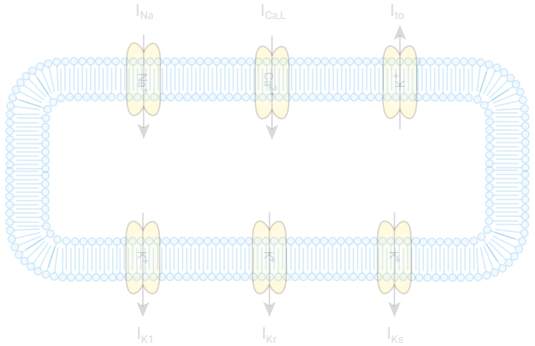

The Forward Problem of Electrocardiology

Bidirectionally Coupled Electromechanics

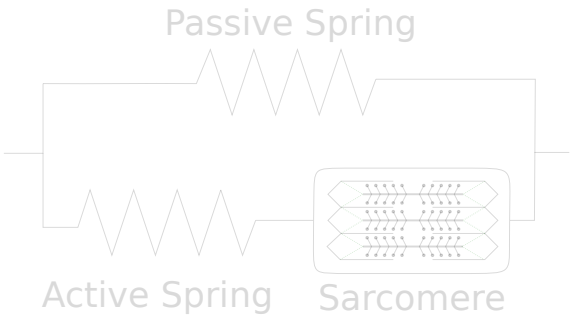

Cardiac Anatomy

Schematic with Vascular System

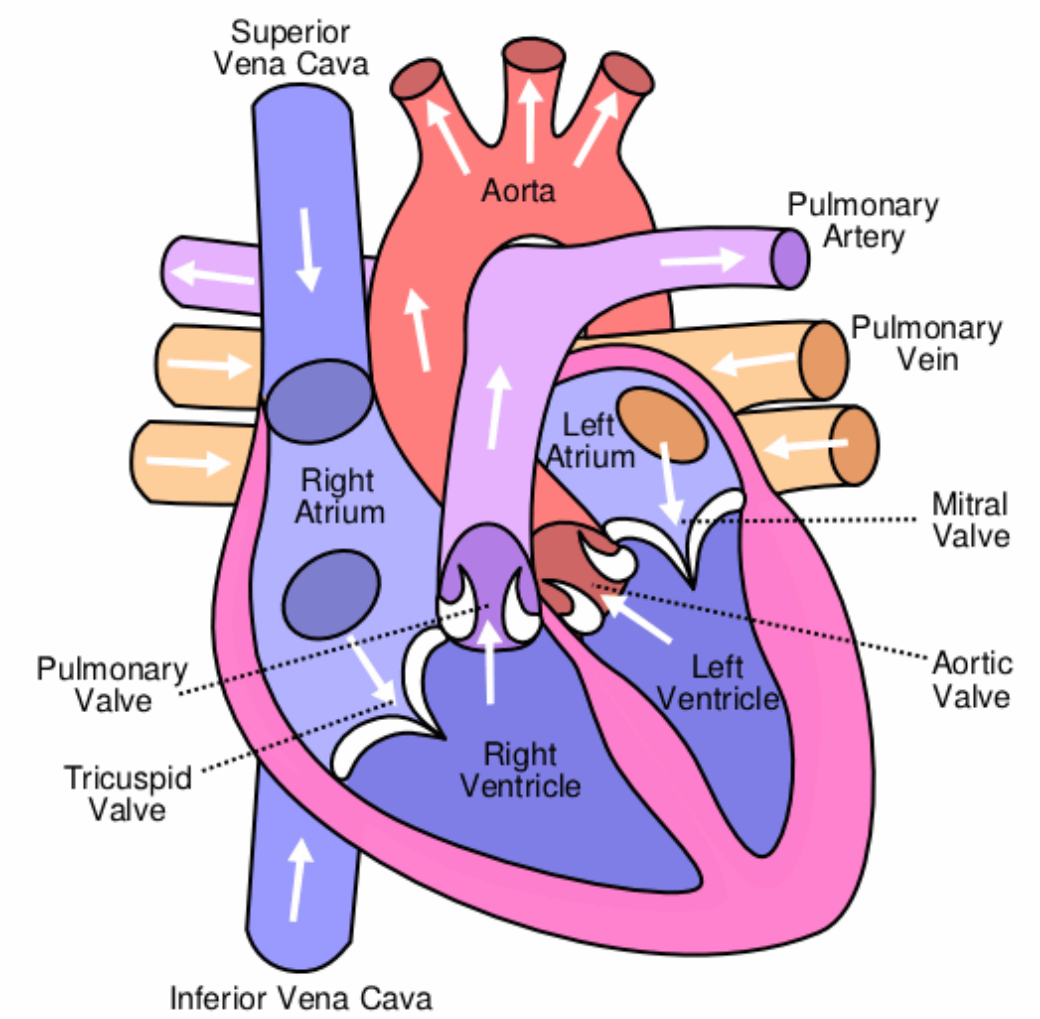

Kjetil Lenes (Wikipedia)

Long Axis Cine MRI (Swine)

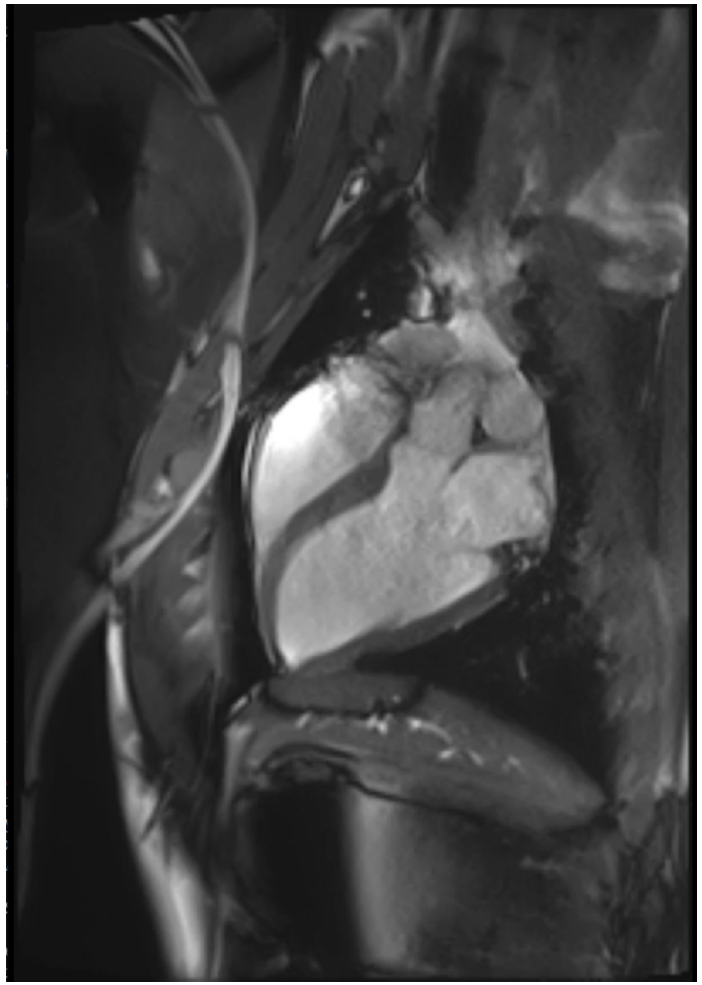

Luigi Perotti

Cardiac Microstructure

Measured Fiber Field (Rabbit)

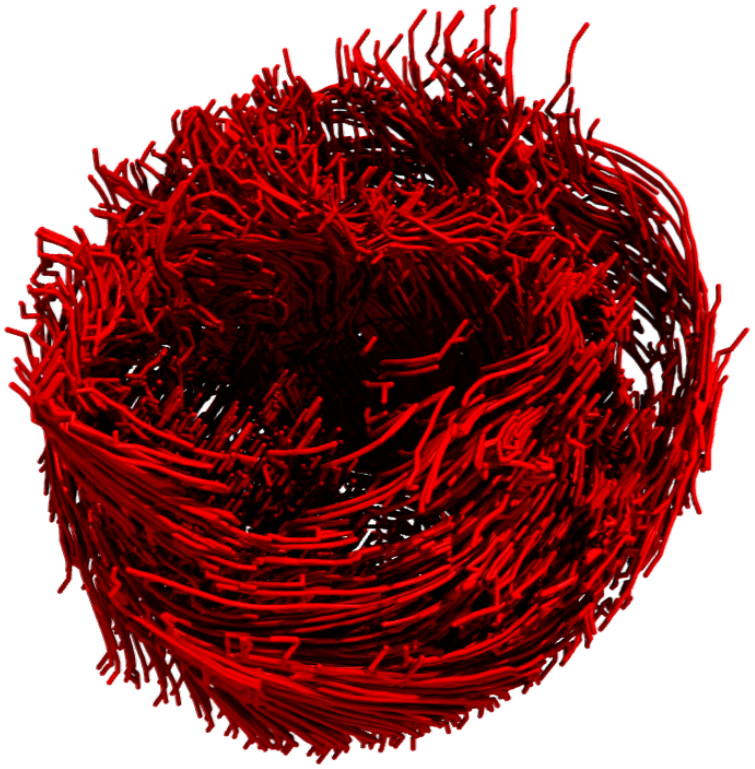

Derived from Krishnamoorthi et al. [2014]

Microstructure Orgranization

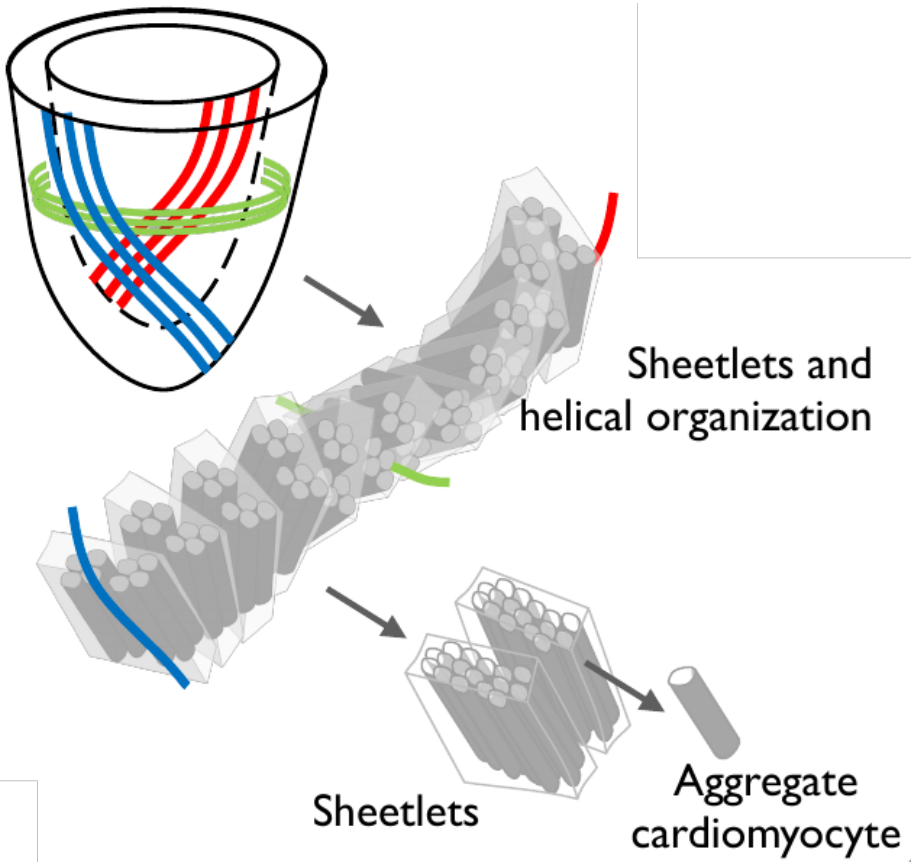

Kevin Moulin

Cardiac Conduction System

Purkinje Network in Ventricles

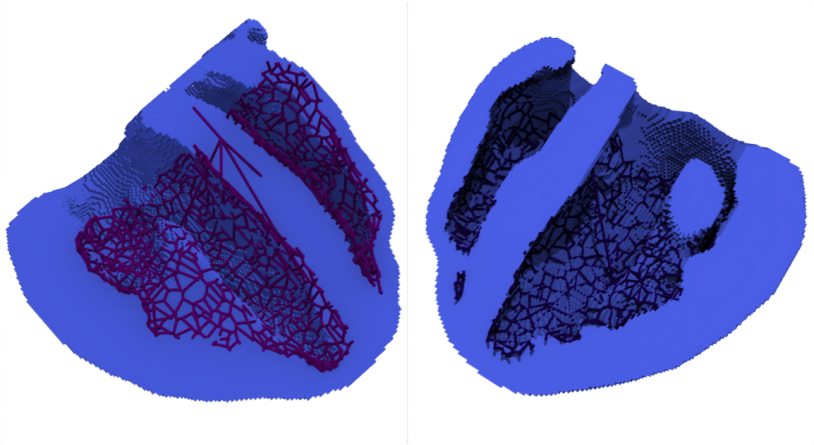

Schematic Conduction System

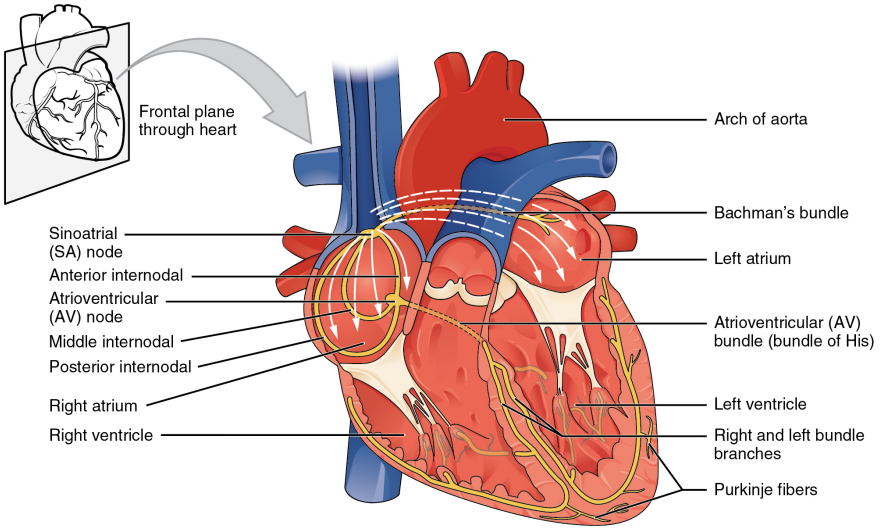

OpenStax College (Wikipedia)

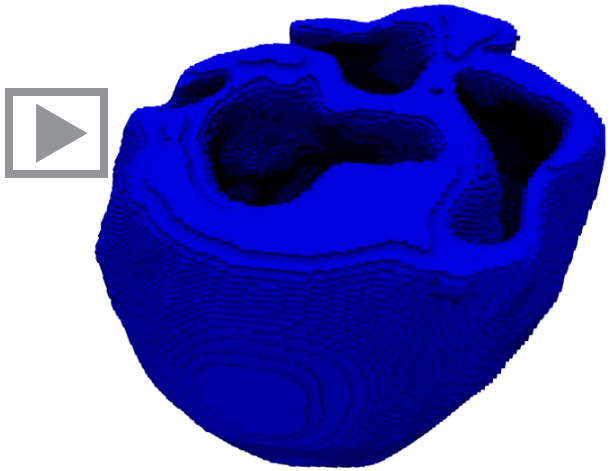

Overview

Basic Cardiac Anatomy and Function

Cardiac Electrophysiology

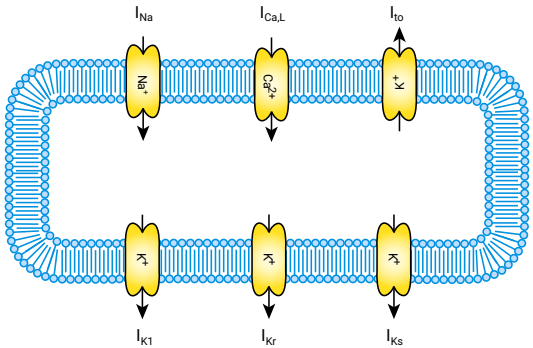

The Forward Problem of Electrocardiology

Bidirectionally Coupled Electromechanics

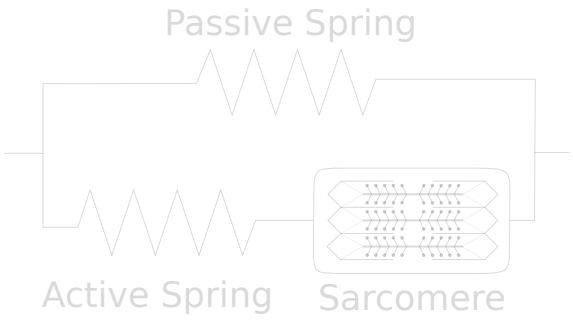

Governing Equations: Bidomain Model

Tung [1978]

Cable Model

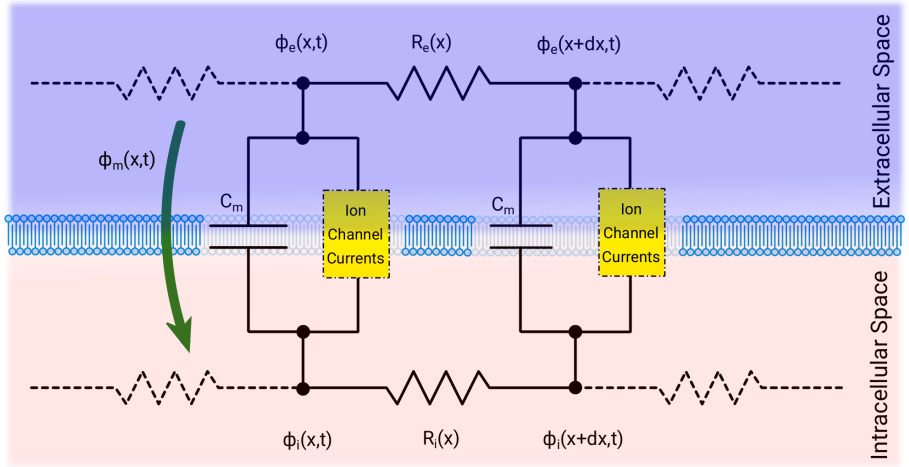

Extension to multiple dimensions

➔ bidomain model

- φ_i intracellular potential
- φ_e extracellular potential
- $\varphi_\mathrm{m} \coloneqq \varphi_\mathrm{i} - \varphi_\mathrm{e}$ transmembrane potential
- $\boldsymbol{R}_\mathrm{i}, \boldsymbol{R}_\mathrm{e}, \boldsymbol{R}_\mathrm{b}$ resistance tensors
- $\boldsymbol{\kappa}_\mathrm{i}, \boldsymbol{\kappa}_\mathrm{e}, \boldsymbol{\kappa}_\mathrm{b}$ conductivity tensors
- C_m membrane capacitance
- χ relative membrane surface area
- $\boldsymbol{s}$ cellular state variables

$$
\begin{aligned}
\chi C_\mathrm{m} \partial_t \varphi_\mathrm{m} &= \nabla \cdot \boldsymbol{\kappa}_\mathrm{i} \nabla \varphi_\mathrm{m} + \nabla \cdot \boldsymbol{\kappa}_\mathrm{i} \nabla \varphi_\mathrm{e} - \chi I_\mathrm{ion}(\varphi_\mathrm{m}, \boldsymbol{s}) - \chi I_\mathrm{stim}(t) && \text{in } \Omega_\mathbb{H} \times (0, T] \\
0 &= \nabla \cdot \boldsymbol{\kappa}_\mathrm{i} \nabla \varphi_\mathrm{m} + \nabla \cdot (\boldsymbol{\kappa}_\mathrm{e} + \boldsymbol{\kappa}_\mathrm{i}) \nabla \varphi_\mathrm{e} && \text{in } \Omega_\mathbb{H} \times (0, T] \\
\partial_t \boldsymbol{s} &= \boldsymbol{g}(\varphi_\mathrm{m}, \boldsymbol{s}) && \text{in } \Omega_\mathbb{H} \times (0, T] \\
0 &= \boldsymbol{n} \cdot \boldsymbol{\kappa}_\mathrm{i} \nabla \varphi_\mathrm{i} && \text{on } \partial\Omega_\mathbb{H} \times (0, T] \\
0 &= \boldsymbol{n} \cdot \boldsymbol{\kappa}_\mathrm{e} \nabla \varphi_\mathrm{e} && \text{on } \partial\Omega_\mathbb{H}^\mathrm{n} \times (0, T] \\
0 &= \varphi_\mathrm{e} && \text{on } \partial\Omega_\mathbb{H}^\mathrm{g} \times (0, T]
\end{aligned}
$$

Numerical Treatment via Operator Splitting Schemes

See e.g. Qu and Garfinkel (1999)

$$
\begin{aligned}
\chi C_\mathrm{m} \partial_t \varphi_\mathrm{m} &= \nabla \cdot \boldsymbol{\kappa}_\mathrm{i} \nabla \varphi_\mathrm{m} + \nabla \cdot \boldsymbol{\kappa}_\mathrm{i} \nabla \varphi_\mathrm{e} && -\chi I_\mathrm{ion}(\varphi_\mathrm{m}, \boldsymbol{s}) - \chi I_\mathrm{stim}(\boldsymbol{x}, t) \\
0 &= \nabla \cdot \boldsymbol{\kappa}_\mathrm{i} \nabla \varphi_\mathrm{m} + \nabla \cdot (\boldsymbol{\kappa}_\mathrm{e} + \boldsymbol{\kappa}_\mathrm{i}) \nabla \varphi_\mathrm{e} && \\
\underbrace{\partial_t \boldsymbol{s}}_{\mathcal{M}\boldsymbol{u}} &= \underbrace{\qquad\qquad\qquad\qquad\qquad\qquad}_{\mathcal{A}\boldsymbol{u}} && \underbrace{\boldsymbol{g}(\varphi_\mathrm{m}, \boldsymbol{s}, t)}_{\mathcal{B}(\boldsymbol{u},t)}
\end{aligned}
$$

➔ Decouples problem into linear PDAE ($\mathcal{A}$) and nonlinear, pointwise ODEs ($\mathcal{B}$)

Numerical Treatment via Operator Splitting Schemes

See e.g. Qu and Garfinkel (1999)

$$
\begin{aligned}
\chi C_\mathrm{m}\partial_t\varphi_\mathrm{m} &= \nabla\cdot\boldsymbol{\kappa}_\mathrm{i}\nabla\varphi_\mathrm{m} + \nabla\cdot\boldsymbol{\kappa}_\mathrm{i}\nabla\varphi_\mathrm{e} && -\chi I_\mathrm{ion}(\varphi_\mathrm{m},\boldsymbol{s}) - \chi I_\mathrm{stim}(\boldsymbol{x},t)\\
0 &= \nabla\cdot\boldsymbol{\kappa}_\mathrm{i}\nabla\varphi_\mathrm{m} + \nabla\cdot(\boldsymbol{\kappa}_\mathrm{e}+\boldsymbol{\kappa}_\mathrm{i})\nabla\varphi_\mathrm{e} &&\\
\underbrace{\partial_t\boldsymbol{s}}_{\mathcal{M}\boldsymbol{u}} &= \underbrace{\qquad\qquad\qquad\qquad\qquad\qquad}_{\mathcal{A}\boldsymbol{u}} && \underbrace{\boldsymbol{g}(\varphi_\mathrm{m},\boldsymbol{s},t)}_{\mathcal{B}(\boldsymbol{u},t)}
\end{aligned}
$$

➔ Decouples problem into linear PDAE ($\mathcal{A}$) and nonlinear, pointwise ODEs ($\mathcal{B}$)

First order Lie-Trotter-Godunov scheme

1. Solve $\mathcal{M}\boldsymbol{u} = \mathcal{A}\boldsymbol{u}$ on $[t_n, t_{n+1}]$
2. Solve $\mathcal{M}\boldsymbol{u} = \mathcal{B}(\boldsymbol{u},t)$ on $[t_n, t_{n+1}]$ with solution of 1. as initial condition

Numerical Treatment via Operator Splitting Schemes

See e.g. Qu and Garfinkel (1999)

$$
\begin{aligned}
\chi C_\mathrm{m}\partial_t\varphi_\mathrm{m} &= \nabla\cdot\boldsymbol{\kappa}_\mathrm{i}\nabla\varphi_\mathrm{m} + \nabla\cdot\boldsymbol{\kappa}_\mathrm{i}\nabla\varphi_\mathrm{e} && -\chi I_\mathrm{ion}(\varphi_\mathrm{m},\boldsymbol{s}) - \chi I_\mathrm{stim}(\boldsymbol{x},t)\\
0 &= \nabla\cdot\boldsymbol{\kappa}_\mathrm{i}\nabla\varphi_\mathrm{m} + \nabla\cdot(\boldsymbol{\kappa}_\mathrm{e}+\boldsymbol{\kappa}_\mathrm{i})\nabla\varphi_\mathrm{e} &&\\
\underbrace{\partial_t\boldsymbol{s}}_{\mathcal{M}\boldsymbol{u}} &= \underbrace{\qquad\qquad\qquad\qquad\qquad\qquad}_{\mathcal{A}\boldsymbol{u}} && \underbrace{\boldsymbol{g}(\varphi_\mathrm{m},\boldsymbol{s},t)}_{\mathcal{B}(\boldsymbol{u},t)}
\end{aligned}
$$

➔ Decouples problem into linear PDAE ($\mathcal{A}$) and nonlinear, pointwise ODEs ($\mathcal{B}$)

First order Lie-Trotter-Godunov scheme

1. Solve $\mathcal{M}\boldsymbol{u} = \mathcal{A}\boldsymbol{u}$ on $[t_n, t_{n+1}]$
2. Solve $\mathcal{M}\boldsymbol{u} = \mathcal{B}(\boldsymbol{u},t)$ on $[t_n, t_{n+1}]$ with solution of 1. as initial condition

➔ Consistency successfully tested via Niederer benchmark (Niederer et al. [2011])

Monodomain Model

Simplifying, unphysiological assumption $\boldsymbol{\kappa}_\mathrm{i} = \lambda \boldsymbol{\kappa}_\mathrm{e}$ and define $\tilde{\boldsymbol{\kappa}} := \frac{\lambda}{1+\lambda}\boldsymbol{\kappa}_\mathrm{i}$

$$
\begin{aligned}
\chi C_\mathrm{m} \partial_t \varphi_\mathrm{m} &= \nabla \cdot \tilde{\boldsymbol{\kappa}} \nabla \varphi_\mathrm{m} - \chi I_\mathrm{ion}(\varphi_\mathrm{m}, \boldsymbol{s}) - \chi I_\mathrm{stim}(t) && \text{in } \Omega_\mathbb{H} \times (0, T] \\
\partial_t \boldsymbol{s} &= \boldsymbol{g}(\varphi_\mathrm{m}, \boldsymbol{s}) && \text{in } \Omega_\mathbb{H} \times (0, T] \\
0 &= \boldsymbol{n} \cdot \tilde{\boldsymbol{\kappa}} \nabla \varphi_\mathrm{m} && \text{on } \partial\Omega_\mathbb{H} \times (0, T]
\end{aligned}
$$

transmembranepotential φ_m

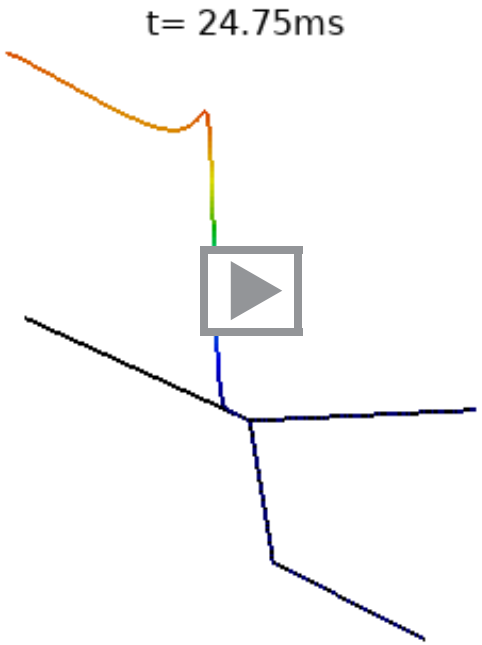

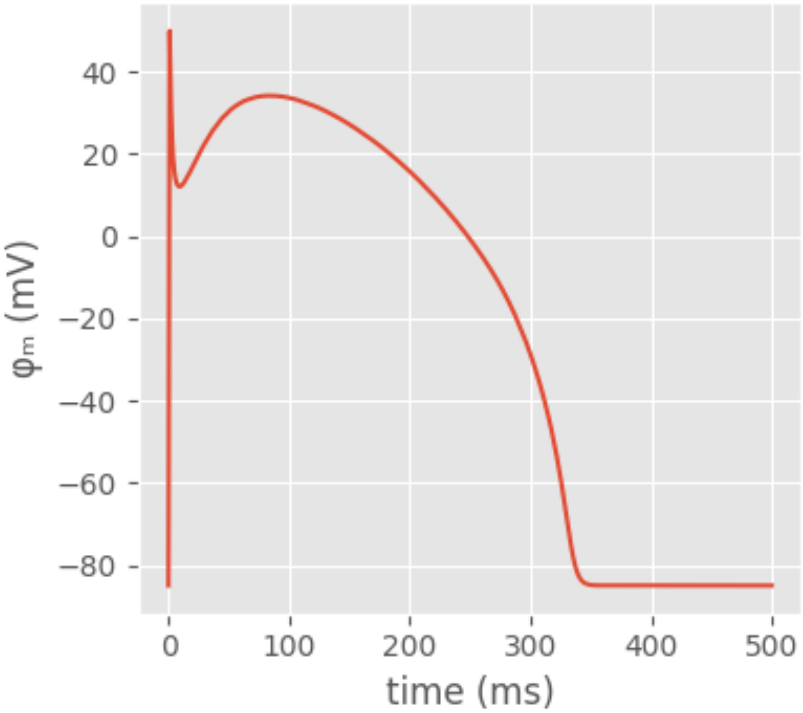

Monodomain Model

Simplifying, unphysiological assumption $\boldsymbol{\kappa}_\mathrm{i} = \lambda \boldsymbol{\kappa}_\mathrm{e}$ and define $\tilde{\boldsymbol{\kappa}} := \frac{\lambda}{1+\lambda}\boldsymbol{\kappa}_\mathrm{i}$

$$
\begin{aligned}
\chi C_\mathrm{m} \partial_t \varphi_\mathrm{m} &= \nabla \cdot \tilde{\boldsymbol{\kappa}} \nabla \varphi_\mathrm{m} - \chi I_\mathrm{ion}(\varphi_\mathrm{m}, \boldsymbol{s}) - \chi I_\mathrm{stim}(t) && \text{in } \Omega_\mathbb{H} \times (0, T] \\
\partial_t \boldsymbol{s} &= \boldsymbol{g}(\varphi_\mathrm{m}, \boldsymbol{s}) && \text{in } \Omega_\mathbb{H} \times (0, T] \\
0 &= \boldsymbol{n} \cdot \tilde{\boldsymbol{\kappa}} \nabla \varphi_\mathrm{m} && \text{on } \partial\Omega_\mathbb{H} \times (0, T]
\end{aligned}
$$

transmembranepotential φ_m

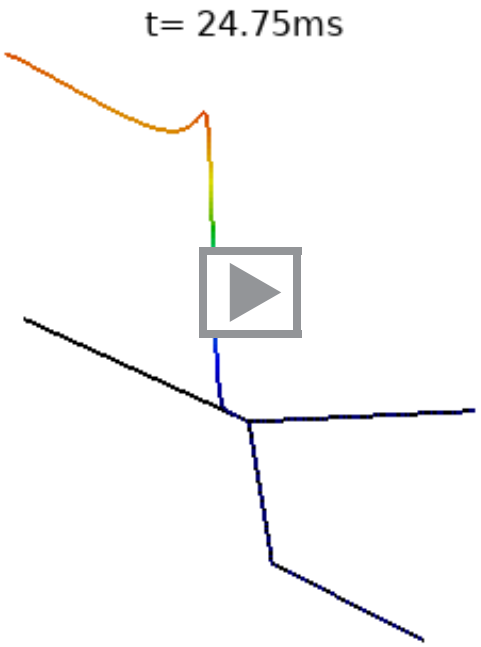

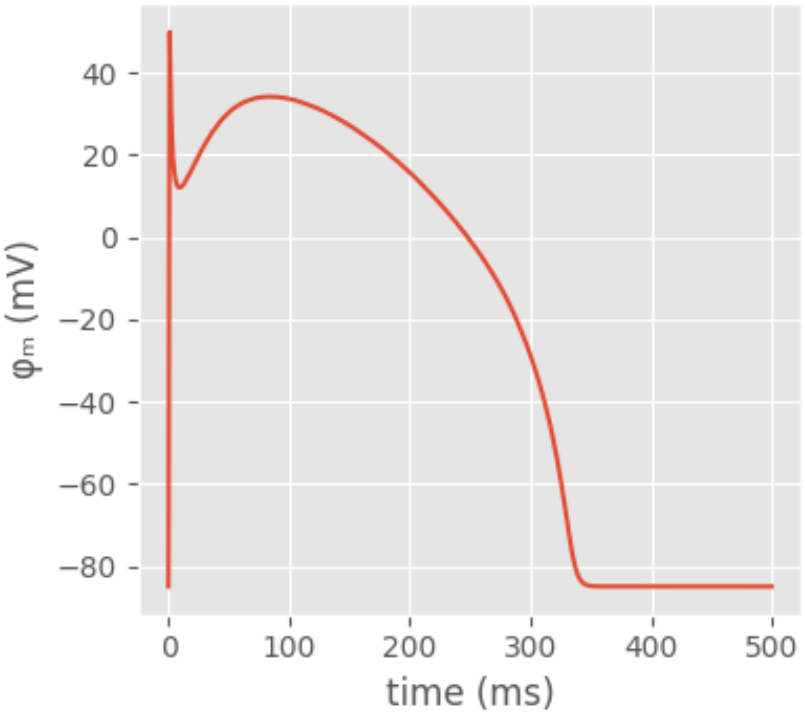

Note: Coudière, et al. [2014] : Mean harmonic tensor for physiological conductivities suitable

Preasymptotic Behavior in Cardiac Electrophysiology

Adopted from Pezzuto, Hake and Sundnes [2015]

- Continuous (Galerkin) discretization with equidistant partitioning of $\Omega_{\mathbb{H}} \approx \mathbb{R}$
- Bistable reaction: $I_{\text{ion}} = a(\varphi_{\text{m}} - \varphi_{\text{rest}})(\varphi_{\text{m}} - \varphi_{\text{thresh}})(\varphi_{\text{m}} - \varphi_{\text{depol}})$
- No cellular state variables
- Initiate traveling wave and measure asymptotic wave speed c_h numerically

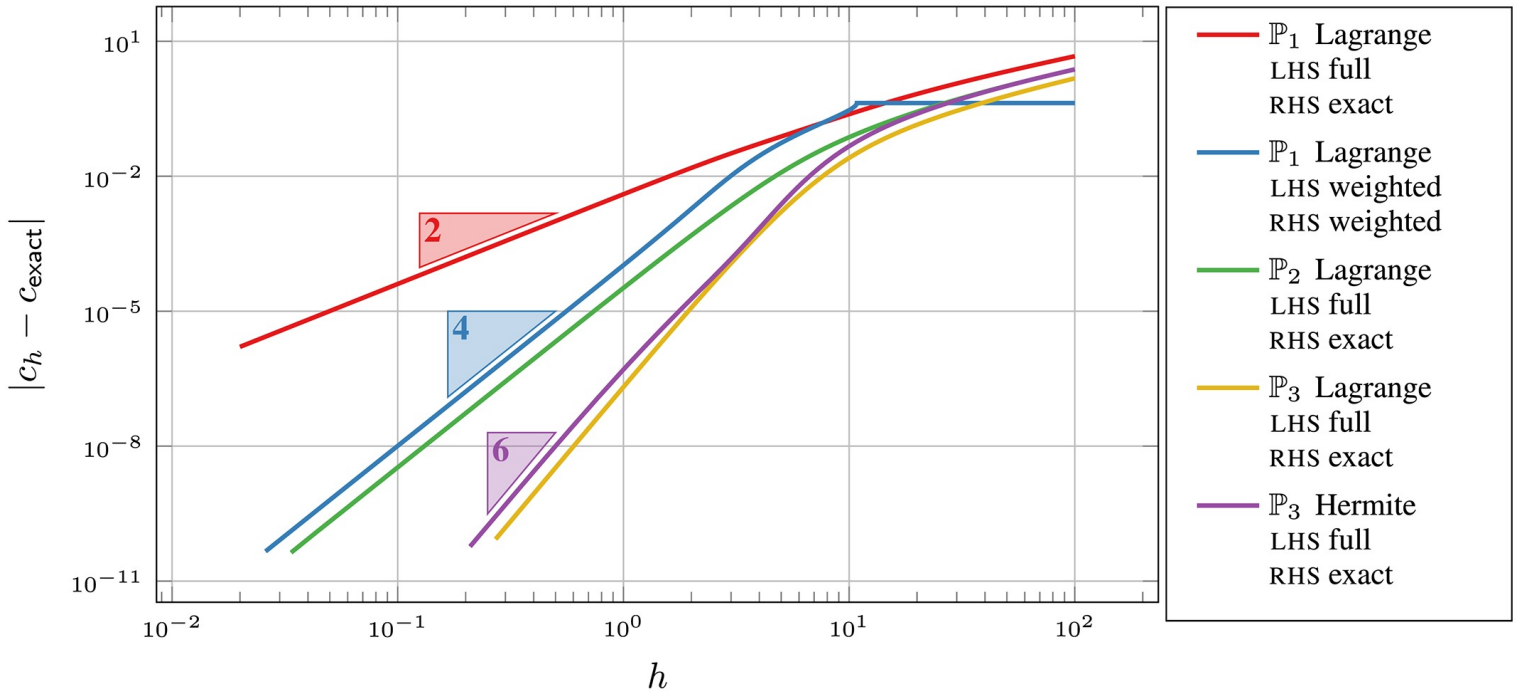

➔ Linear convergence in preasymptotic regieme (boundary layer theory)

Adaptive Mesh Refinement via Kelly Error Indicator

Kelly et al. [1983] **and** Gago et al. [1983]

Tree-based AMR

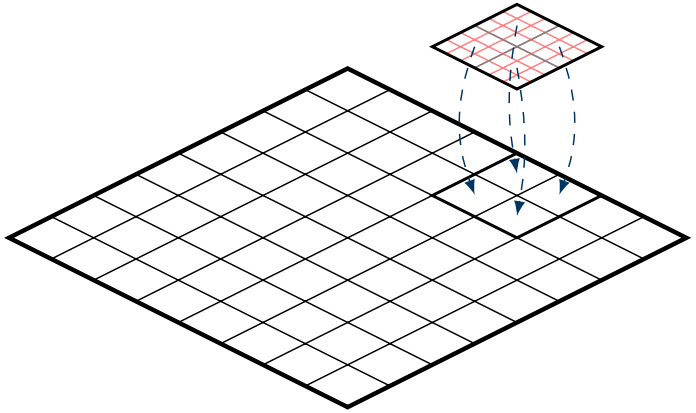

- Only wavefront needs fine grid
  ➔ Use coarse grid and refine only on wavefront
- Local nonconforming refinement
- Coarsening by tracking refinement with tree data structure
- Using MFEM (Anderson et al. [2019])

- Kelly error indicator

$$err_E(\varphi_\mathrm{m})^2 \approx h_E \int_{\partial E} [[\tilde{\boldsymbol{\kappa}} \nabla \varphi_\mathrm{m}]]^2 \mathrm{d}\boldsymbol{S}$$

- $[[\cdot]]$ indicates jump operator
- Threshold-based de-/refinement
- Should perform reasonably based on a posteriori error estimates (c.f. Ratti et al. [2019])

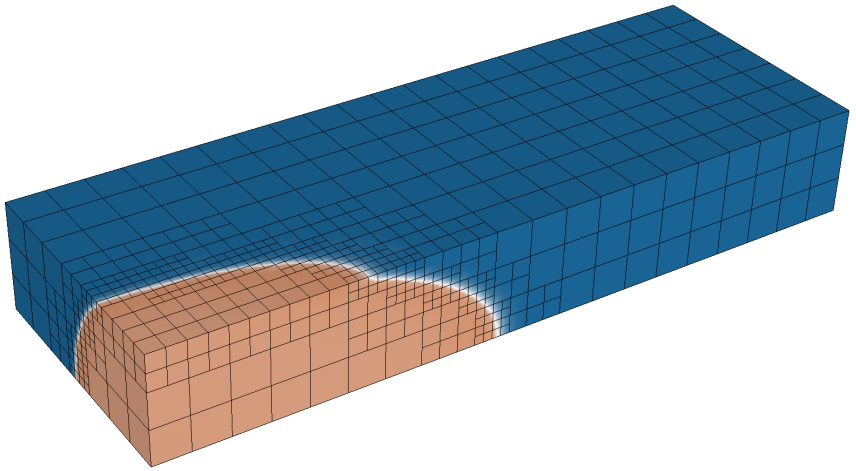

Ionic Model: PCG Canine Ventricular Cardiomyocyte

Pathmanathan, Cordeiro and Gray [2019]

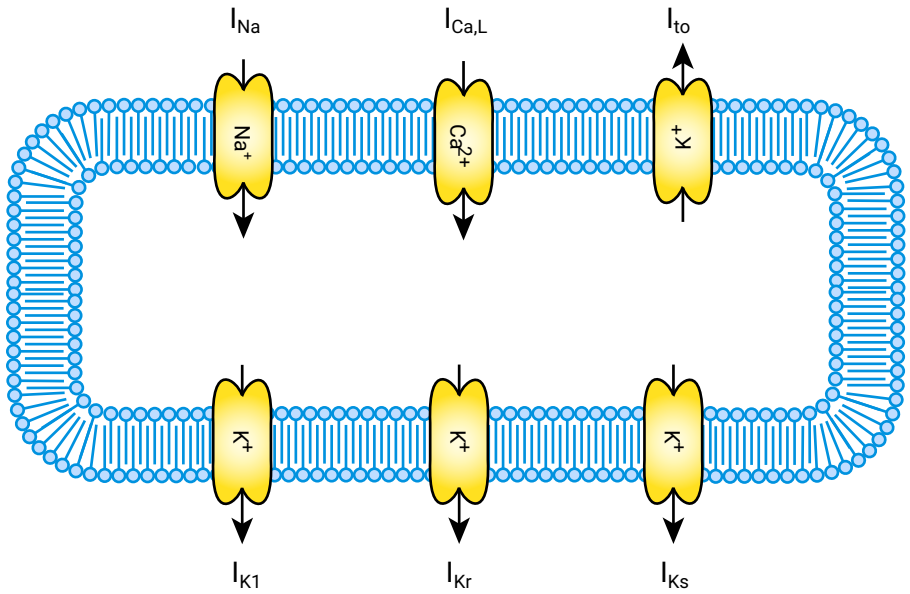

- Only 6 dynamic ion channel states
- 36 parameters
- Fitted using exclusively canine data
- Physiologically plausible dynamics
- Nice numerical properties
- Undergone extensive UQ and GSA

➔ parallel lines of batteries and nonlinear (voltage-modulated) resistors

$$I_{\text{ion}}(\varphi_{\text{m}}, \boldsymbol{s}) = \sum_{i \in \{\text{Na,K1,to,CaL,Kr,Ks}\}} \underbrace{g_i p_i(\varphi_{\text{m}}, \boldsymbol{s})\,(\varphi_{\text{m}} - E_i)}_{:= I_i}$$

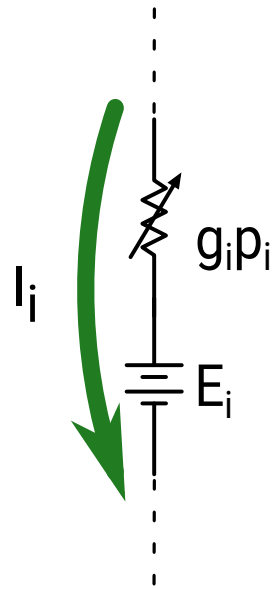

where the resistors' states evolution is described with

$$\mathbf{g}(\varphi_{\text{m}}, \boldsymbol{s}) = \mathbf{A}(\varphi_{\text{m}})\boldsymbol{s} + \mathbf{b}(\varphi_{\text{m}})$$

with nonlinear functions $\mathbf{A}$ and $\mathbf{b}$. Details in Pathmanathan et al. [2019].

Spiral Wave Break Benchmark

Ogiermann, Perotti and Balzani. To be submitted.

- scaling g_{to} up ➔ instable spiral waves Landaw et al. [2021].
- Initial condition: Gradients in φ_{m} and fast gates (c.f. Pathmanathan et al. [2021])

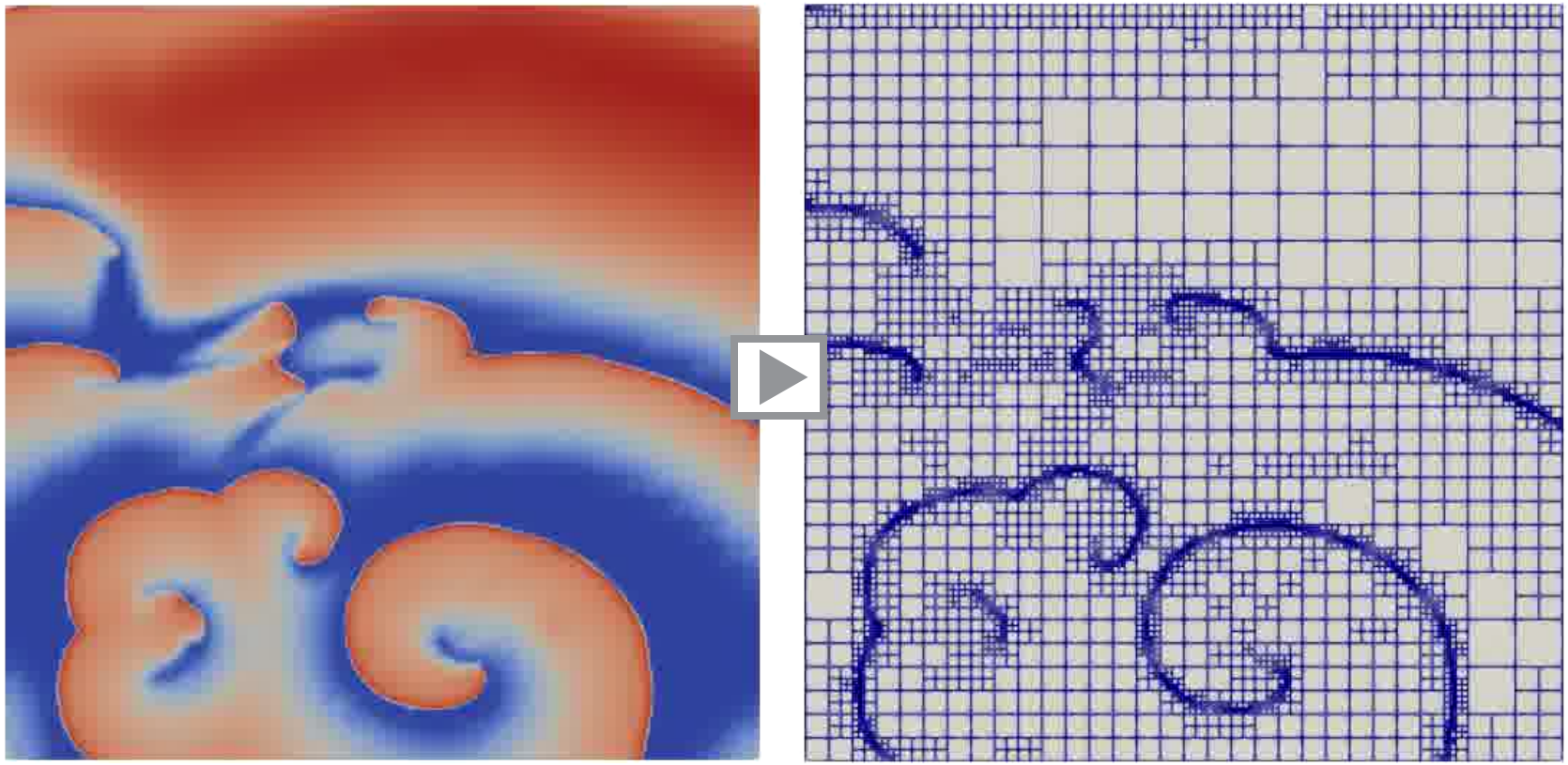

➔ AMR simulation $\approx 4\times$ faster than non-adaptive

Overview

Basic Cardiac Anatomy and Function

Cardiac Electrophysiology

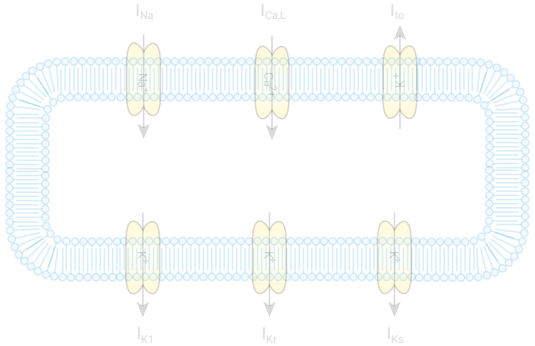

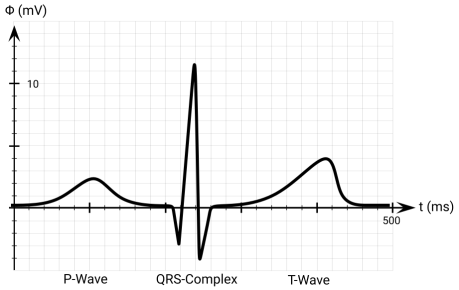

The Forward Problem of Electrocardiology

Bidirectionally Coupled Electromechanics

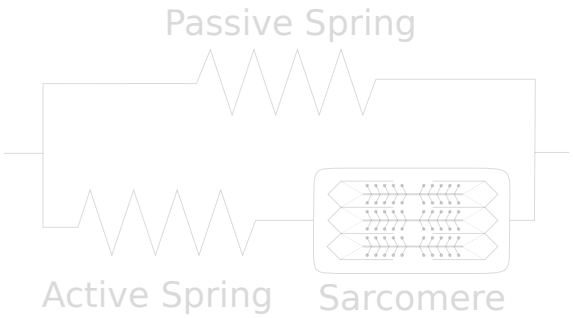

Towards Validation of EP Models at Organ-Level

➔ ECG as a tool to validate EP simulations

➔ Full dataset available (Moss et al. [2022])

Important features of physiological ECG[1]:

- No slurrying or fractionations
- QRS duration and amplitude
- QRS progression
- Positive T-wave with longer rise than fall

Idealized ECG lead

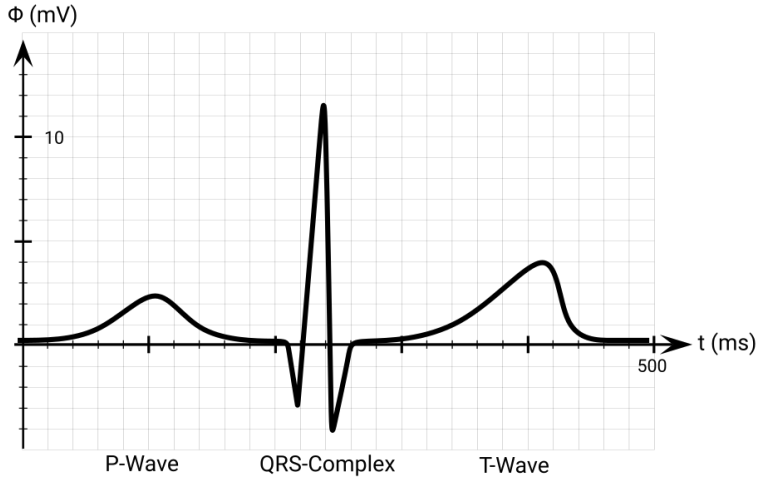

Challenges

- Conductivities are "unknown"
- Measurement of conduction system problematic
- Uncertainty in microstructure
  - ➔ Huge progess recently (e.g. Ennis Lab, Stanford)
- Full simulations computationally demanding
- ECG quite sensitive measure

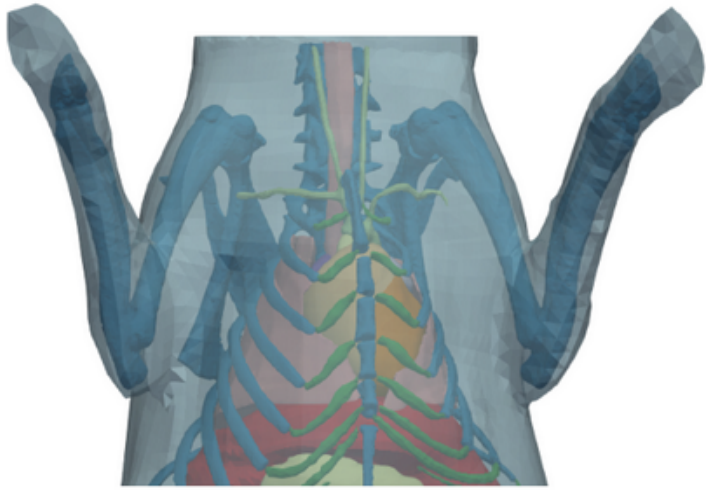

Moss et al. [2022]

[1] Krishnamoorthi et al. [2014]

ECG Modeling

Direct ECG

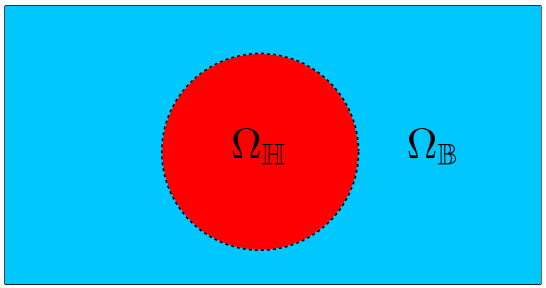

Bidomain model with torso[2]:

$$
\begin{aligned}
\chi C_{\mathrm{m}} \frac{\partial \varphi_{\mathrm{m}}}{\partial t} &= \nabla \cdot \boldsymbol{\kappa}_{\mathrm{i}} \nabla \varphi_{\mathrm{m}} + \nabla \cdot \boldsymbol{\kappa}_{\mathrm{i}} \nabla \varphi_{\mathrm{e}} - \chi I_{\mathrm{ion}}(\varphi_{\mathrm{m}}, \mathbf{s}) - \chi I_{\mathrm{stim}}(t) && \text{in } \Omega_{\mathbb{H}} \\
0 &= \nabla \cdot \boldsymbol{\kappa}_{\mathrm{i}} \nabla \varphi_{\mathrm{m}} + \nabla \cdot (\boldsymbol{\kappa}_{\mathrm{e}} + \boldsymbol{\kappa}_{\mathrm{i}}) \nabla \varphi_{\mathrm{e}} && \text{in } \Omega_{\mathbb{H}} \\
\frac{\partial \mathbf{s}}{\partial t} &= \mathbf{g}(\varphi_{\mathrm{m}}, \mathbf{s}) && \text{in } \Omega_{\mathbb{H}} \\
0 &= \nabla \cdot \kappa_{\mathrm{b}} \nabla \varphi_{\mathrm{b}} && \text{in } \Omega_{\mathbb{B}}
\end{aligned}
$$

[2] Tung [1978]

ECG Modeling

Direct ECG

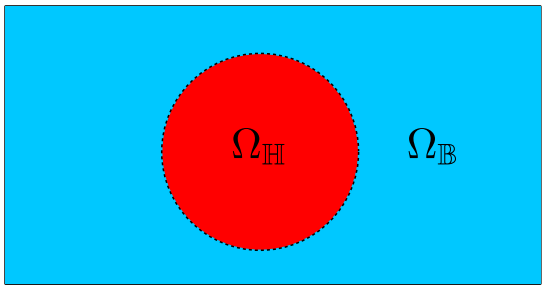

Bidomain model with torso[2]:

$$
\begin{aligned}
\chi C_{\mathrm{m}} \frac{\partial \varphi_{\mathrm{m}}}{\partial t} &= \nabla \cdot \boldsymbol{\kappa}_{\mathrm{i}} \nabla \varphi_{\mathrm{m}} + \nabla \cdot \boldsymbol{\kappa}_{\mathrm{i}} \nabla \varphi_{\mathrm{e}} - \chi I_{\mathrm{ion}}(\varphi_{\mathrm{m}}, \mathbf{s}) - \chi I_{\mathrm{stim}}(t) && \text{in } \Omega_{\mathbb{H}} \\
0 &= \nabla \cdot \boldsymbol{\kappa}_{\mathrm{i}} \nabla \varphi_{\mathrm{m}} + \nabla \cdot (\boldsymbol{\kappa}_{\mathrm{e}} + \boldsymbol{\kappa}_{\mathrm{i}}) \nabla \varphi_{\mathrm{e}} && \text{in } \Omega_{\mathbb{H}} \\
\frac{\partial \mathbf{s}}{\partial t} &= \mathbf{g}(\varphi_{\mathrm{m}}, \mathbf{s}) && \text{in } \Omega_{\mathbb{H}} \\
0 &= \nabla \cdot \kappa_{\mathrm{b}} \nabla \varphi_{\mathrm{b}} && \text{in } \Omega_{\mathbb{B}}
\end{aligned}
$$

[2] Tung [1978]

ECG Modeling

Direct ECG

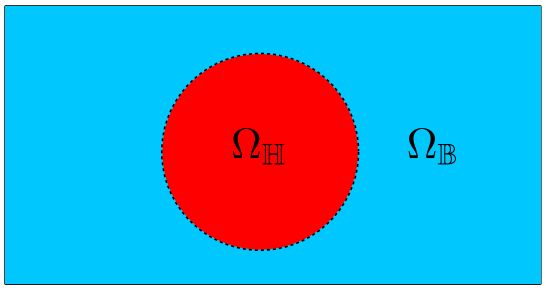

Bidomain model with torso[2]:

$$
\begin{aligned}
\chi C_{\mathrm{m}} \frac{\partial \varphi_{\mathrm{m}}}{\partial t} &= \nabla \cdot \boldsymbol{\kappa}_{\mathrm{i}} \nabla \varphi_{\mathrm{m}} + \nabla \cdot \boldsymbol{\kappa}_{\mathrm{i}} \nabla \varphi_{\mathrm{e}} - \chi I_{\mathrm{ion}}(\varphi_{\mathrm{m}}, \mathbf{s}) - \chi I_{\mathrm{stim}}(t) && \text{in } \Omega_{\mathbb{H}} \\
0 &= \nabla \cdot \boldsymbol{\kappa}_{\mathrm{i}} \nabla \varphi_{\mathrm{m}} + \nabla \cdot (\boldsymbol{\kappa}_{\mathrm{e}} + \boldsymbol{\kappa}_{\mathrm{i}}) \nabla \varphi_{\mathrm{e}} && \text{in } \Omega_{\mathbb{H}} \\
\frac{\partial \mathbf{s}}{\partial t} &= \mathbf{g}(\varphi_{\mathrm{m}}, \mathbf{s}) && \text{in } \Omega_{\mathbb{H}} \\
0 &= \nabla \cdot \kappa_{\mathrm{b}} \nabla \varphi_{\mathrm{b}} && \text{in } \Omega_{\mathbb{B}}
\end{aligned}
$$

[2] Tung [1978]

ECG Modeling

Direct ECG

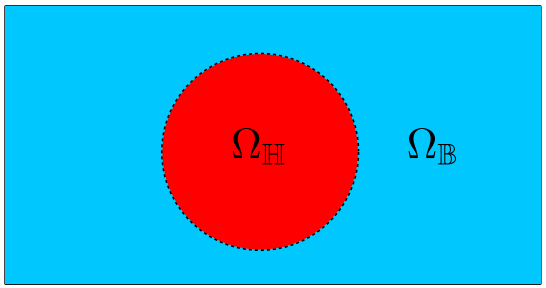

Bidomain model with torso[2]:

$$
\begin{aligned}
\chi C_{\mathrm{m}} \frac{\partial \varphi_{\mathrm{m}}}{\partial t} &= \nabla \cdot \boldsymbol{\kappa}_{\mathrm{i}} \nabla \varphi_{\mathrm{m}} + \nabla \cdot \boldsymbol{\kappa}_{\mathrm{i}} \nabla \varphi_{\mathrm{e}} - \chi I_{\mathrm{ion}}(\varphi_{\mathrm{m}}, \mathbf{s}) - \chi I_{\mathrm{stim}}(t) && \text{in } \Omega_{\mathbb{H}} \\
0 &= \nabla \cdot \boldsymbol{\kappa}_{\mathrm{i}} \nabla \varphi_{\mathrm{m}} + \nabla \cdot (\boldsymbol{\kappa}_{\mathrm{e}} + \boldsymbol{\kappa}_{\mathrm{i}}) \nabla \varphi_{\mathrm{e}} && \text{in } \Omega_{\mathbb{H}} \\
\frac{\partial \mathbf{s}}{\partial t} &= \mathbf{g}(\varphi_{\mathrm{m}}, \mathbf{s}) && \text{in } \Omega_{\mathbb{H}} \\
0 &= \nabla \cdot \kappa_{\mathrm{b}} \nabla \varphi_{\mathrm{b}} && \text{in } \Omega_{\mathbb{B}}
\end{aligned}
$$

➔ Perfect transmission condition between φ_{e} and φ_{b}

[2] Tung [1978]

ECG Modeling

Direct ECG

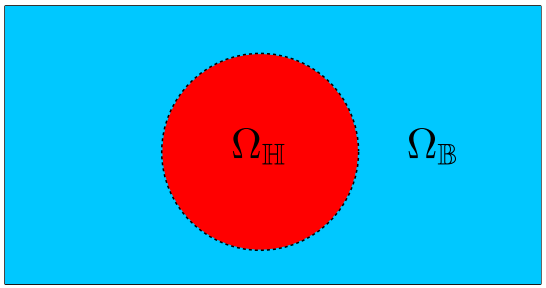

Bidomain model with torso[2]:

$$
\begin{aligned}
\chi C_{\mathrm{m}} \frac{\partial \varphi_{\mathrm{m}}}{\partial t} &= \nabla \cdot \boldsymbol{\kappa}_{\mathrm{i}} \nabla \varphi_{\mathrm{m}} + \nabla \cdot \boldsymbol{\kappa}_{\mathrm{i}} \nabla \varphi_{\mathrm{e}} - \chi I_{\mathrm{ion}}(\varphi_{\mathrm{m}}, \mathbf{s}) - \chi I_{\mathrm{stim}}(t) && \text{in } \Omega_{\mathbb{H}} \\
0 &= \nabla \cdot \boldsymbol{\kappa}_{\mathrm{i}} \nabla \varphi_{\mathrm{m}} + \nabla \cdot (\boldsymbol{\kappa}_{\mathrm{e}} + \boldsymbol{\kappa}_{\mathrm{i}}) \nabla \varphi_{\mathrm{e}} && \text{in } \Omega_{\mathbb{H}} \\
\frac{\partial \mathbf{s}}{\partial t} &= \mathbf{g}(\varphi_{\mathrm{m}}, \mathbf{s}) && \text{in } \Omega_{\mathbb{H}} \\
0 &= \nabla \cdot \kappa_{\mathrm{b}} \nabla \varphi_{\mathrm{b}} && \text{in } \Omega_{\mathbb{B}}
\end{aligned}
$$

➔ Perfect transmission condition between φ_{e} and φ_{b}

➔ **Gold standard** in cardiac EP modeling

[2] Tung [1978]

ECG Modeling

Direct ECG

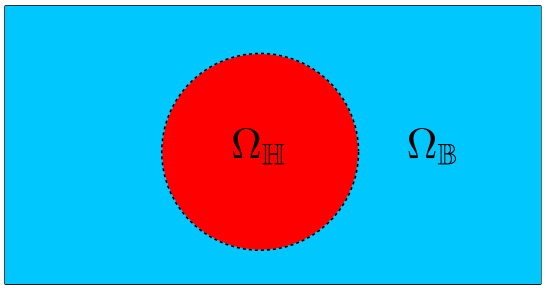

Bidomain model with torso[2]:

$$
\begin{aligned}
\chi C_{\mathrm{m}} \frac{\partial \varphi_{\mathrm{m}}}{\partial t} &= \nabla \cdot \boldsymbol{\kappa}_{\mathrm{i}} \nabla \varphi_{\mathrm{m}} + \nabla \cdot \boldsymbol{\kappa}_{\mathrm{i}} \nabla \varphi_{\mathrm{e}} - \chi I_{\mathrm{ion}}(\varphi_{\mathrm{m}}, \mathbf{s}) - \chi I_{\mathrm{stim}}(t) && \text{in } \Omega_{\mathbb{H}} \\
0 &= \nabla \cdot \boldsymbol{\kappa}_{\mathrm{i}} \nabla \varphi_{\mathrm{m}} + \nabla \cdot (\boldsymbol{\kappa}_{\mathrm{e}} + \boldsymbol{\kappa}_{\mathrm{i}}) \nabla \varphi_{\mathrm{e}} && \text{in } \Omega_{\mathbb{H}} \\
\frac{\partial \mathbf{s}}{\partial t} &= \mathbf{g}(\varphi_{\mathrm{m}}, \mathbf{s}) && \text{in } \Omega_{\mathbb{H}} \\
0 &= \nabla \cdot \kappa_{\mathrm{b}} \nabla \varphi_{\mathrm{b}} && \text{in } \Omega_{\mathbb{B}}
\end{aligned}
$$

➔ Perfect transmission condition between φ_{e} and φ_{b}

➔ **Gold standard** in cardiac EP modeling

➔ Most prominent ECG models identifiable as **special cases** of this model

[2] Tung [1978]

ECG Modeling

Direct ECG

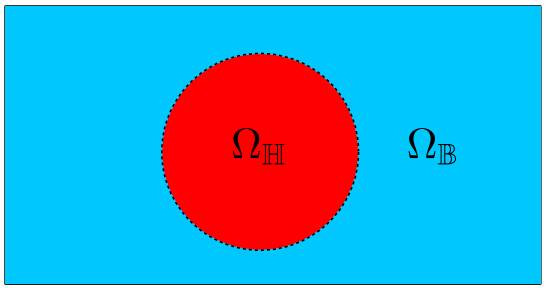

Bidomain model with torso[2]:

$$
\begin{aligned}
\chi C_{\mathrm{m}} \frac{\partial \varphi_{\mathrm{m}}}{\partial t} &= \nabla \cdot \boldsymbol{\kappa}_{\mathrm{i}} \nabla \varphi_{\mathrm{m}} + \nabla \cdot \boldsymbol{\kappa}_{\mathrm{i}} \nabla \varphi_{\mathrm{e}} - \chi I_{\mathrm{ion}}(\varphi_{\mathrm{m}}, \mathbf{s}) - \chi I_{\mathrm{stim}}(t) && \text{in } \Omega_{\mathbb{H}} \\
0 &= \nabla \cdot \boldsymbol{\kappa}_{\mathrm{i}} \nabla \varphi_{\mathrm{m}} + \nabla \cdot (\boldsymbol{\kappa}_{\mathrm{e}} + \boldsymbol{\kappa}_{\mathrm{i}}) \nabla \varphi_{\mathrm{e}} && \text{in } \Omega_{\mathbb{H}} \\
\frac{\partial \mathbf{s}}{\partial t} &= \mathbf{g}(\varphi_{\mathrm{m}}, \mathbf{s}) && \text{in } \Omega_{\mathbb{H}} \\
0 &= \nabla \cdot \kappa_{\mathrm{b}} \nabla \varphi_{\mathrm{b}} && \text{in } \Omega_{\mathbb{B}}
\end{aligned}
$$

➔ Perfect transmission condition between φ_{e} and φ_{b}

➔ **Gold standard** in cardiac EP modeling

➔ Most prominent ECG models identifiable as **special cases** of this model

➔ ECG results in evaluating φ_{b}

[2] Tung [1978]

Computational Experiments on a Transmural Wedge

Ogiermann, Perotti and Balzani. [2022] PAMM.

- Uniform cell type everywhere
- Perfectly insulating surrounding
- Rotating fiber distribution

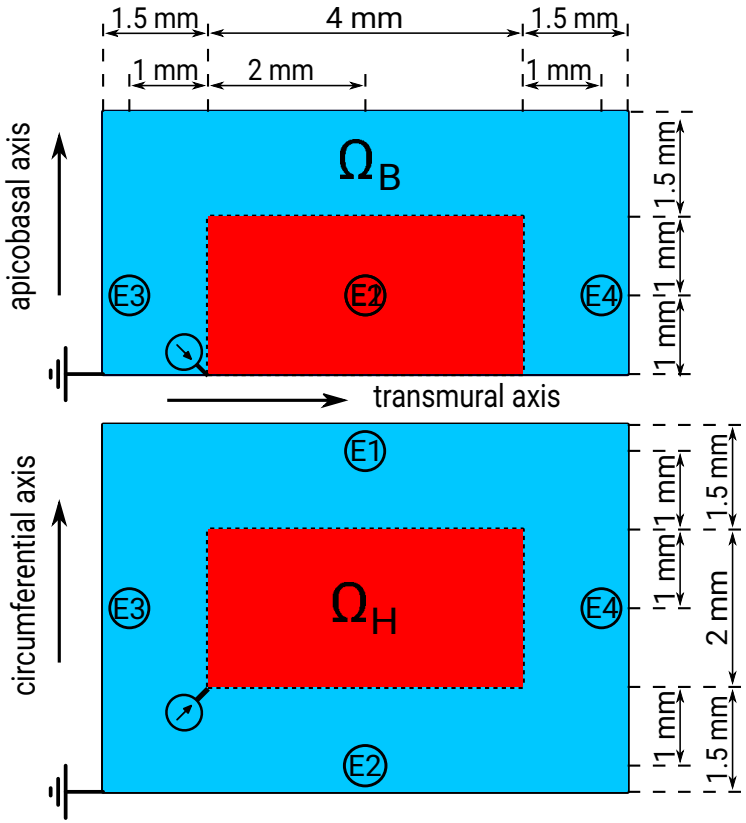

mS/mm	$\kappa_{i,f}$	$\kappa_{i,s}$	$\kappa_{i,n}$	$\kappa_{e,f}$	$\kappa_{e,s}$	$\kappa_{e,n}$
Clerk (1976)	0.17	0.019	0.019	0.63	0.24	0.24
Roberts et al. (1978)	0.28	0.026	0.026	0.22	0.13	0.13
Roberts et al. (1982)	0.34	0.06	0.06	0.12	0.08	0.08
MacLachlan et al. (2005)	0.3	0.1	0.032	0.2	0.17	0.14
Hooks (2007)	0.26	0.026	0.008	0.26	0.25	0.11
Johnston (2016)	0.24	0.035	0.008	0.24	0.2	0.11

PCG2019 vs TNNP2006 Cell Model

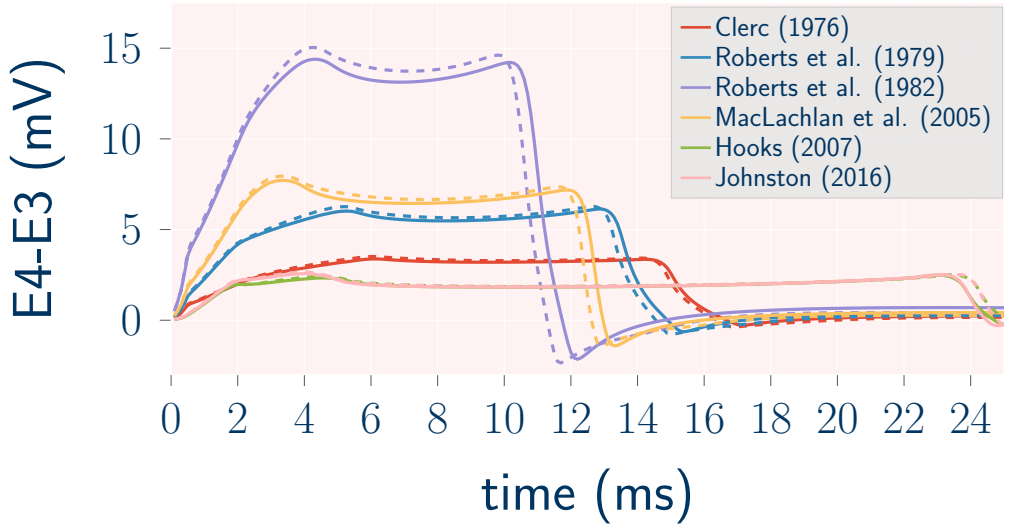

PCG 2019 (Solid Line) ; TNNP 2006 (Dashed Line)

Computational Experiments on a Transmural Wedge

Ogiermann, Perotti and Balzani. [2022] PAMM.

- Uniform cell type everywhere
- Perfectly insulating surrounding
- Rotating fiber distribution

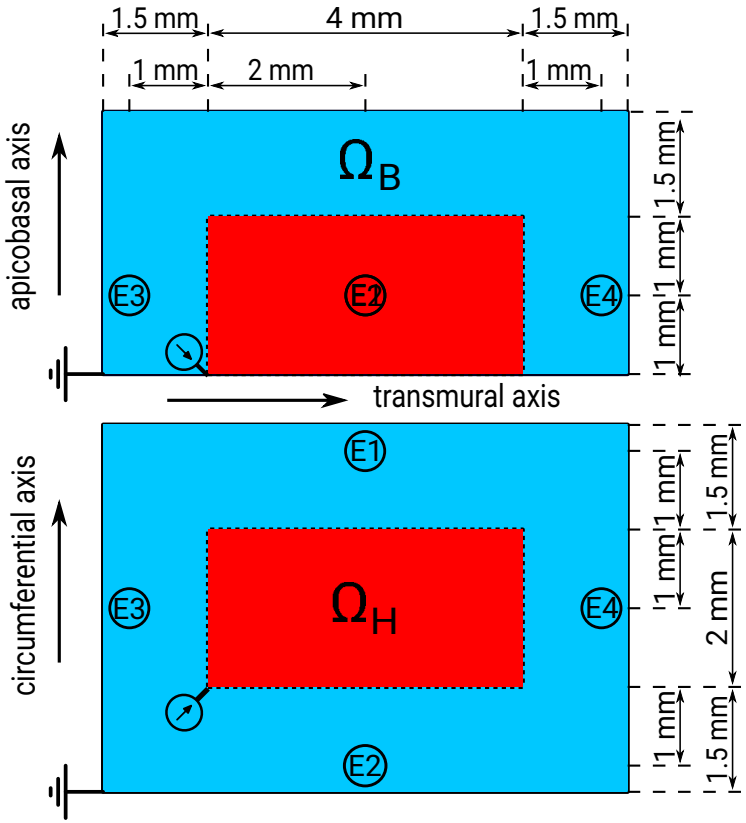

mS/mm	$\kappa_{i,f}$	$\kappa_{i,s}$	$\kappa_{i,n}$	$\kappa_{e,f}$	$\kappa_{e,s}$	$\kappa_{e,n}$
Clerk (1976)	0.17	0.019	0.019	0.63	0.24	0.24
Roberts et al. (1978)	0.28	0.026	0.026	0.22	0.13	0.13
Roberts et al. (1982)	0.34	0.06	0.06	0.12	0.08	0.08
MacLachlan et al. (2005)	0.3	0.1	0.032	0.2	0.17	0.14
Hooks (2007)	0.26	0.026	0.008	0.26	0.25	0.11
Johnston (2016)	0.24	0.035	0.008	0.24	0.2	0.11

PCG2019 vs TNNP2006 Cell Model

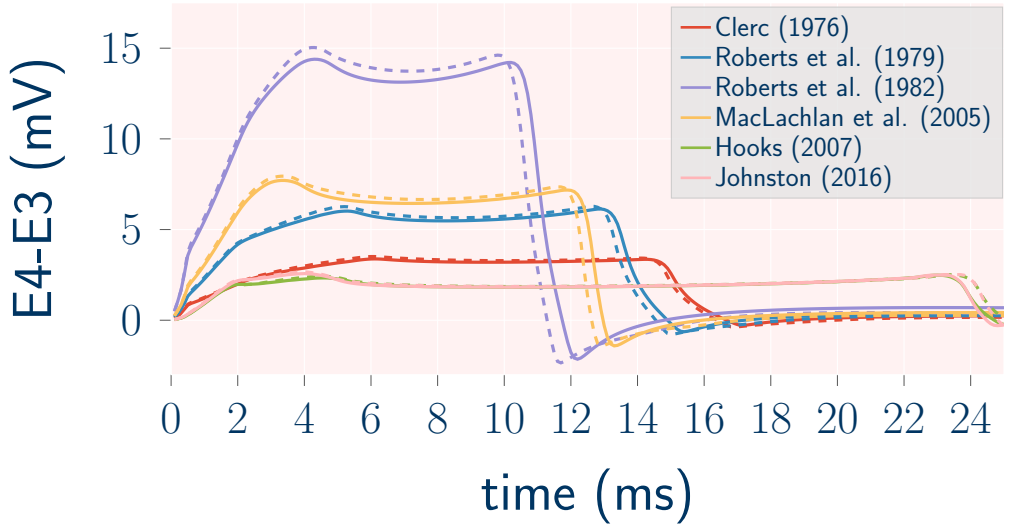

PCG 2019 (Solid Line) ; TNNP 2006 (Dashed Line)

➔ Direct ECG sensitive to conductivities, but insensitive to chosen cell model.

Adaptive Time Stepping via Reaction-Tangent Controller

Ogiermann, Perotti and Balzani. [2021] Submitted.

Observation for space-time discretization error (c.f. Spiteri and Ziaratgahi. [2016])

$$||\boldsymbol{u}_{\mathcal{E}} - \hat{\tilde{\boldsymbol{u}}}_{\mathcal{E}}|| \leq \underbrace{err_{\text{spatial}}}_{\approx 0} + err_{\text{split}} + \underbrace{err_{\text{time step diffusion}}}_{\approx 0} + \underbrace{err_{\text{time step ionic}}}_{\approx 0} .$$

We also know that

$$err_{\text{split}} \sim ||I_{\text{ion}}(\hat{\tilde{\boldsymbol{u}}}(\bullet,\bullet),\bullet) + I_{\text{stim}}(\bullet,\bullet)||_{L_\infty([t_n,t_{n+1}],L_\infty(\Omega))}$$

and make the choice

$$\Delta t_{n+1} = \sigma(||I_{\text{ion}}(\hat{\tilde{\boldsymbol{u}}}(\bullet,\bullet),\bullet) + I_{\text{stim}}(\bullet,\bullet)||_{L_\infty([t_n,t_{n+1}],L_\infty(\Omega))})$$

where σ is a sigmoidal function

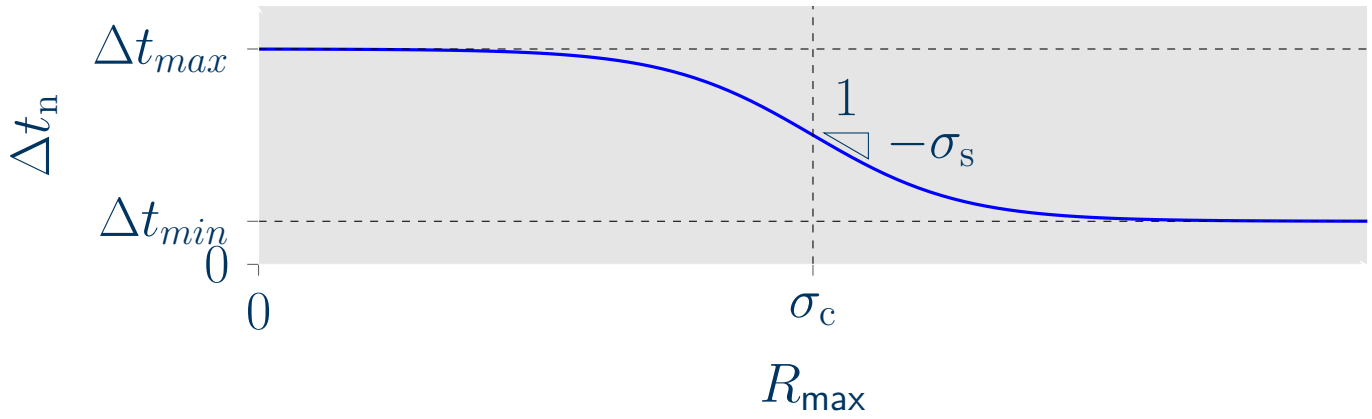

Adaptive Time Stepping via Reaction-Tangent Controller

Ogiermann, Perotti and Balzani. [2021] Submitted.

Trajectory at Material Point

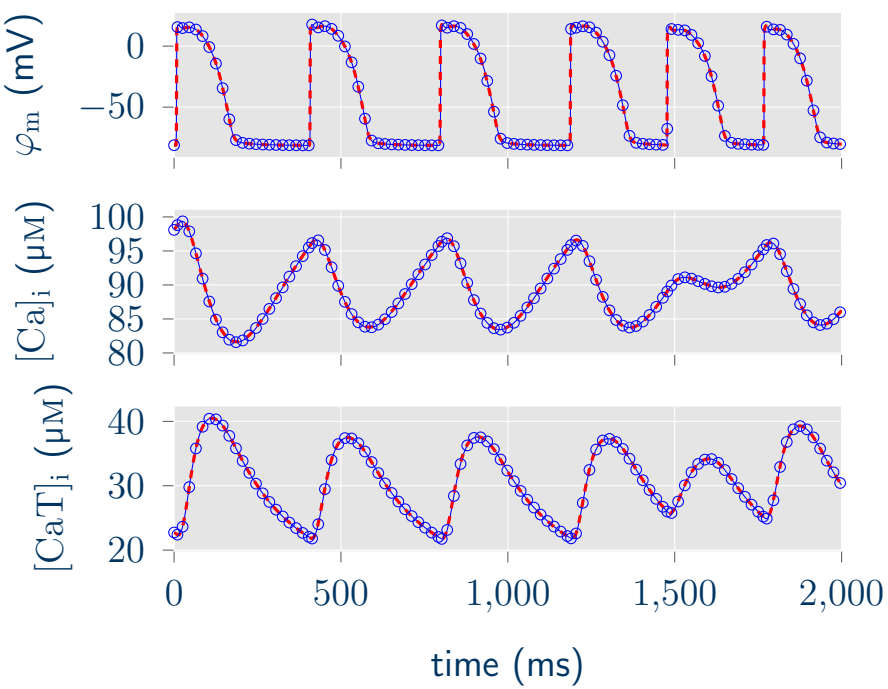

Activation Time Errors

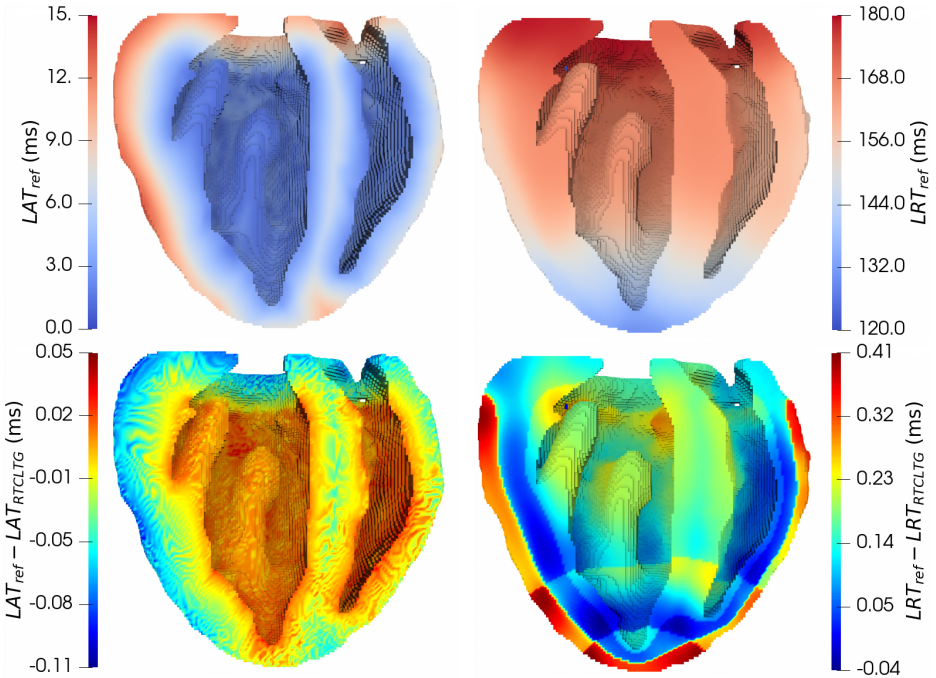

Space-Time Errors

φ_m	$L_2([0,350];L_2(\Omega))$	0.2045
	$L_2([0,350];H^1(\Omega))$	0.4196
	$L_\infty([0,350];L_2(\Omega))$	0.0182
	$L_\infty([0,350];H^1(\Omega))$	0.0968
	$L_\infty([0,350];L_\infty(\Omega))$	0.0052

- OS generalization of Whiteley [2007]
- Qu and Garfinkel [1999] adaptive Euler
- Simple to implement
- $\approx 10\times$ speedup for normal cycles
- Limited use for fibrillation studies

Purkinje Network Coupling

Based on Algorithm by Vergara et al. [2016]

1. Solve EP problem on $\Omega_{\mathbb{H}}$ with stimulus

$$\tilde{I}_{\text{stim}} = I_{\text{stim},\mathbb{H}} + \sum_j \frac{1}{\text{vol}(\mathcal{B}_j)} \mathcal{N}_{\mathbb{H}}(\mathcal{B}_j) \gamma_j^k$$

2. Solve EP problem on $\Omega_{\mathbb{P}}$ with stimulus

$$\tilde{I}_{\text{stim}} = I_{\text{stim},\mathbb{P}} - \sum_j \frac{1}{\text{vol}(\mathcal{B}_j)} \mathcal{N}_{\mathbb{P}}(\mathcal{B}_j) \gamma_j^k$$

3. Match nodes in $\mathcal{B}_j$
4. Update gap voltages $\gamma_1^{k+1}, \ldots$

$$\gamma_j^{k+1} = \frac{\varphi_{\text{m},\mathbb{P}}(\boldsymbol{x}_j, t) - \frac{1}{\text{vol}(\mathcal{B}_j)} \int_{\mathcal{B}_j} \varphi_{\text{m},\mathbb{H}} \text{d}V}{R_{\text{PMJ}}}$$

5. If $\|\boldsymbol{\gamma}^{k+1} - \boldsymbol{\gamma}^k\| > \varepsilon$ goto 1

Schematic Setup

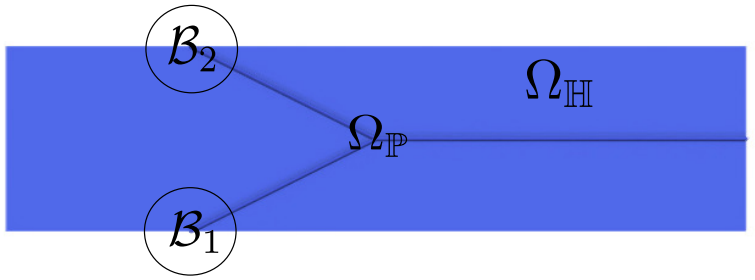

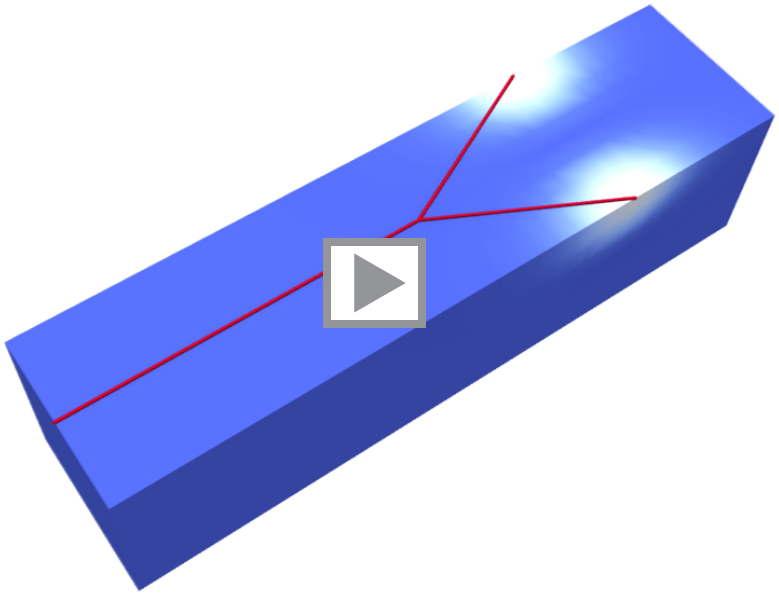

ECG of Biventricular Simulations

Ogiermann, Balzani and Perotti. [2021] LNCS.

Rabbit Heart in Conductive Medium

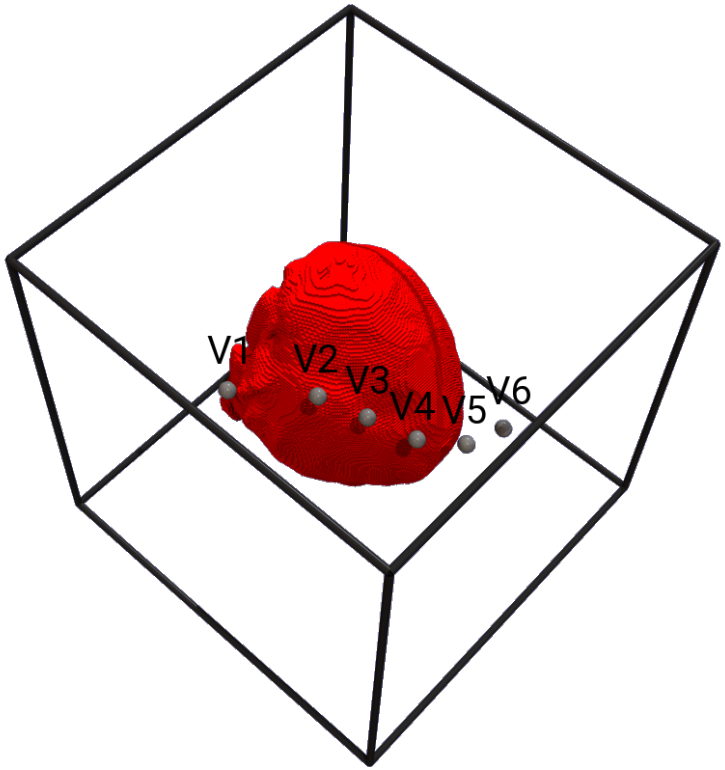

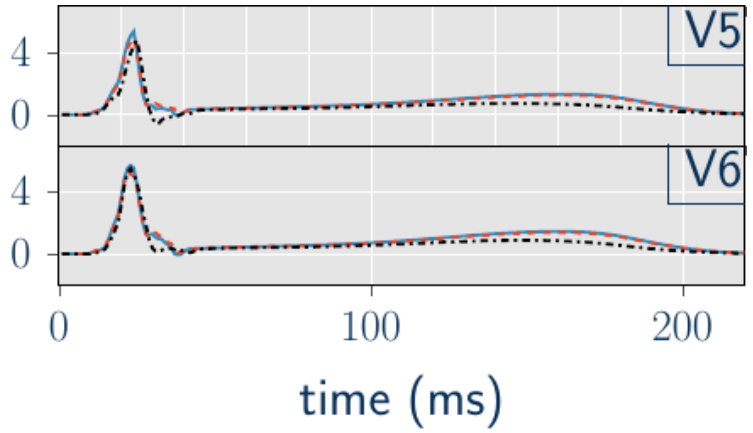

- Activation via Purkinje network
- Utilize measured microstructure from Krishnamoorthi et al. [2014]
- Electrodes placement like clinical setting

➔ Allows investigation of ECG features without torso-associated uncertainties

Overview

Basic Cardiac Anatomy and Function

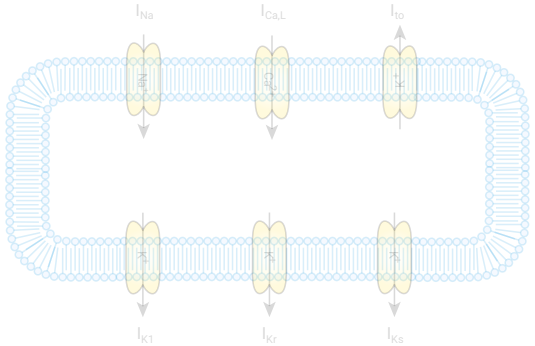

Cardiac Electrophysiology

The Forward Problem of Electrocardiology

Bidirectionally Coupled Electromechanics

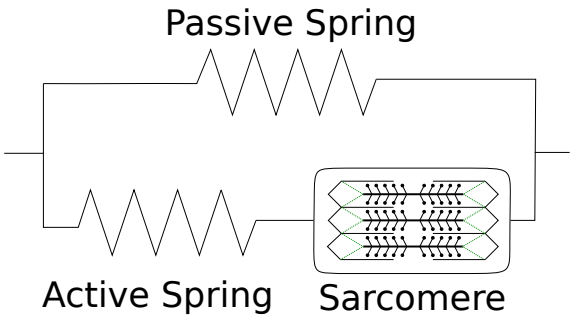

Large Deformations

Kinematics

Displacement

$$\boldsymbol{d} = \boldsymbol{x} - \boldsymbol{X}$$

Deformation gradient

$$\boldsymbol{F} = \mathrm{Grad}\,\boldsymbol{x} = \boldsymbol{I} + \mathrm{Grad}\,\boldsymbol{d}$$

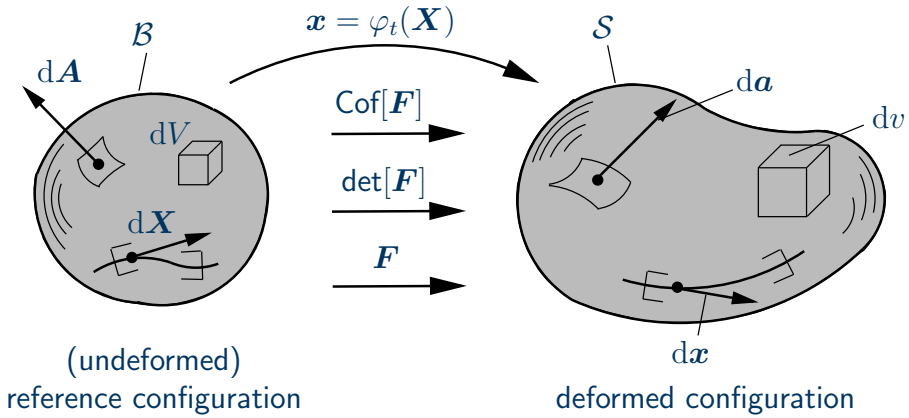

Stress Calculation at Large Strains

The first Piola-Kirchoff stress tensor $\boldsymbol{P}$ can be obtained by differentiation of the strain energy density function $\Psi(\boldsymbol{F})$:

$$\boldsymbol{P} = \frac{\partial \Psi(\boldsymbol{F})}{\partial \boldsymbol{F}}$$

Governing Equations Without Dynamics

$$\nabla \cdot \boldsymbol{P} = \boldsymbol{0}$$

Mechanics: Generalized Hill Model

Göktepe, Menzel and Kuhl [2014]

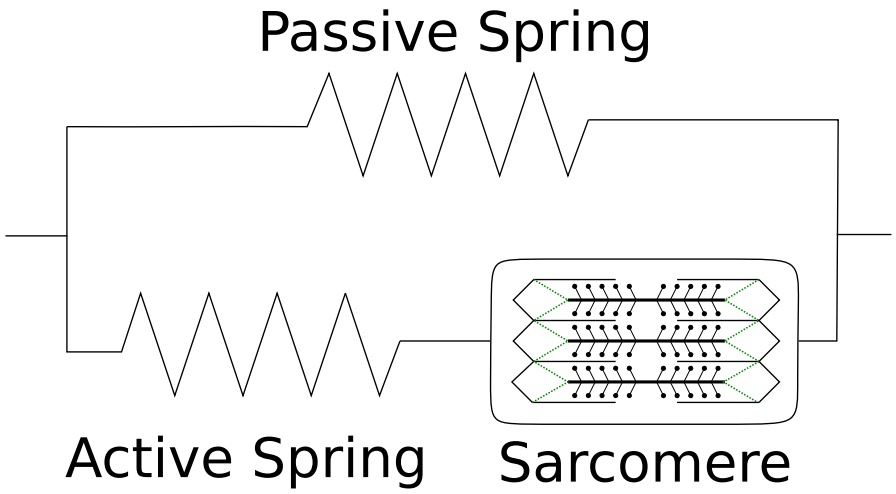

- $\boldsymbol{F} = \boldsymbol{F}^{\mathrm{e}}\boldsymbol{F}^{\mathrm{a}}$
- $\Psi(\boldsymbol{F}, \boldsymbol{F}^{\mathrm{a}}) = \Psi^{\mathrm{passive}}(\boldsymbol{F}) + \Psi^{\mathrm{active}}(\boldsymbol{F}^{\mathrm{e}})$
- $\boldsymbol{F}^{\mathrm{a}} := \sum_{\boldsymbol{m}\in\{\boldsymbol{f},\boldsymbol{s},\boldsymbol{n}\}} \lambda^{\mathrm{a}}_{\boldsymbol{m}} \boldsymbol{m}_0 \otimes \boldsymbol{m}_0$
- Active stretch $\lambda^{\mathrm{a}}_{\boldsymbol{m}}$ (contraction model)
- Fiber stretch $\lambda_{\boldsymbol{f}} = \sqrt{\boldsymbol{F}\boldsymbol{f}_0 \cdot \boldsymbol{F}\boldsymbol{f}_0}$
- $\boldsymbol{C} = \boldsymbol{F}^{\mathrm{T}}\boldsymbol{F}$, $\boldsymbol{C}^{\mathrm{e}} = \boldsymbol{F}^{\mathrm{e}\mathrm{T}}\boldsymbol{F}^{\mathrm{e}}$

➔ Additive split of stress

$$\boldsymbol{P} = \boldsymbol{P}^{\mathrm{passive}}(\boldsymbol{F}) + \boldsymbol{P}^{\mathrm{active}}(\boldsymbol{F}^{\mathrm{e}})$$

➔ $\boldsymbol{P}^{\mathrm{passive}}$ from strain energy density

$$\Psi^{\mathrm{passive}} = \alpha(\bar{I}_1(\boldsymbol{C}) - 3) + U(\det(\boldsymbol{C}))$$

➔ $\boldsymbol{P}^{\mathrm{active}}$ from strain energy density

$$\Psi^{\mathrm{active}} = \frac{\eta}{2}\left(I_{4,\boldsymbol{f}}(\boldsymbol{C}^{\mathrm{e}}) - 1\right)^2$$

➔ Active stretch relation by Pelce [1995]

$$\lambda^{\mathrm{a}}_{\boldsymbol{f}}\left(\overline{[\mathrm{Ca}^{2+}]}_i\right) = \frac{\xi}{1 + f\left(\overline{[\mathrm{Ca}^{2+}]}_i\right)\xi}\lambda^{\mathrm{a}}_{\boldsymbol{f},\max}$$

➔ Incompressibility of the cell

$$\lambda^{\mathrm{a}}_{\boldsymbol{s}} = \lambda^{\mathrm{a}}_{\boldsymbol{n}} = \frac{1}{\sqrt{\lambda^{\mathrm{a}}_{\boldsymbol{f}}}}$$

Ionic Model: Modified PCG Canine Ventricular Cardiomyocyte

Derived from Pathmanathan, Cordeiro and Gray [2019]

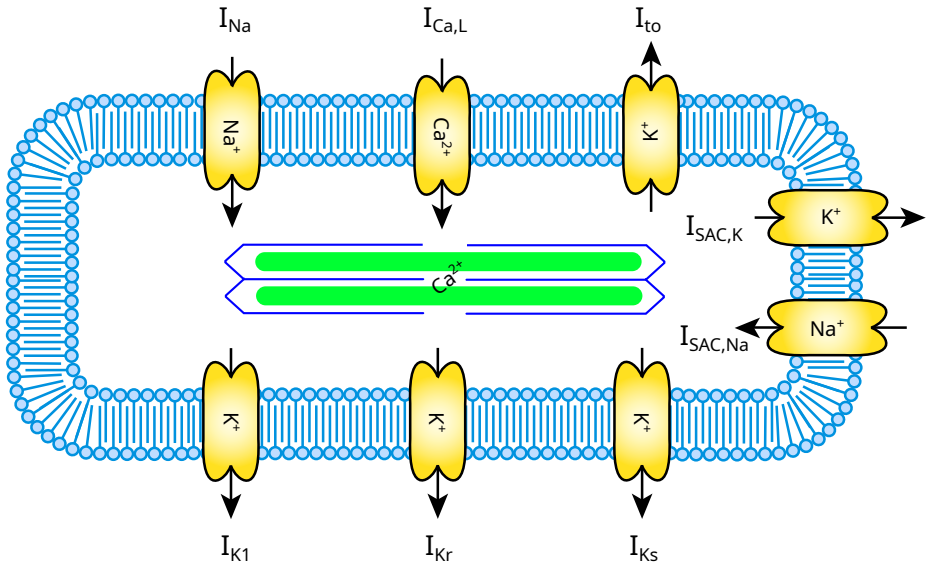

- Minimal calcium dynamics
- Stretch-activated currents
- Hodgkin-Huxley like formulation
- Kinetics from rat data
- Simple to implement
- Useful for verification purposes

$$I_{\text{ion}}(\varphi_{\text{m}}, \boldsymbol{s}, \lambda_{\mathbf{f}}) = \sum_{i \in \{\text{Na,K}\}} I_{\text{SAC},i}(\varphi_{\text{m}}, \lambda_{\mathbf{f}}) + \sum_{i \in \{\text{Na,K1,to,CaL,Kr,Ks}\}} \underbrace{g_i p_i(\varphi_{\text{m}}, \boldsymbol{s})\,(\varphi_{\text{m}} - E_i)}_{:= I_i}$$

I_{SAC} widely used formulation from Niederer and Smith [2007]:

$$I_{\text{SAC},i}(\varphi_{\text{m}}, \lambda_{\mathbf{f}}) = g_{\text{SAC},i} \langle \lambda_{\mathbf{f}} - 1 \rangle (\varphi_{\text{m}} - E_i)$$

Minimal calcium dynamics model with parameters $p_1, p_2, \varphi_{\text{m},0}$:

$$\partial_t [\text{Ca}^{2+}]_{\text{i}} = p_1(\varphi_{\text{m}} - \varphi_{\text{m},0}) - p_2 [\text{Ca}^{2+}]_{\text{i}}$$

Numerical Scheme

Two-Level Operator Splitting

Physical split of full model

$$
\begin{aligned}
\chi C_{\mathrm{m}} \partial_t \varphi_{\mathrm{m}} &= \nabla \cdot \tilde{\boldsymbol{\kappa}} \nabla \varphi_{\mathrm{m}} - \chi I_{\mathrm{ion}}(\varphi_{\mathrm{m}}, \boldsymbol{s}, \lambda_{\boldsymbol{f}}) - \chi I_{\mathrm{stim}}(t) \\
\mathbf{0} &= \nabla \cdot \boldsymbol{P}(\boldsymbol{F}, \boldsymbol{F}^{\mathrm{a}}) \\
\partial_t \boldsymbol{s} &= \boldsymbol{A}(\varphi_{\mathrm{m}}) \boldsymbol{s} + \boldsymbol{b}(\varphi_{\mathrm{m}}) \\
\partial_t [\mathrm{Ca}^{2+}]_{\mathrm{i}} &= \underbrace{}_{\mathcal{M}[\boldsymbol{d}, [\mathrm{Ca}^{2+}]_{\mathrm{i}}]} \underbrace{p_1 \varphi_{\mathrm{m}} - p_2 [\mathrm{Ca}^{2+}]_{\mathrm{i}}}_{\mathcal{E}[\varphi_{\mathrm{m}}, \boldsymbol{d}, \boldsymbol{s}, [\mathrm{Ca}^{2+}]_{\mathrm{i}}]}
\end{aligned}
$$

Reaction-diffusion split of EP Model $\mathcal{E}$

$$
\begin{aligned}
\chi C_{\mathrm{m}} \partial_t \varphi_{\mathrm{m}} &= \nabla \cdot \tilde{\boldsymbol{\kappa}} \nabla \varphi_{\mathrm{m}} \quad -\chi I_{\mathrm{ion}}(\varphi_{\mathrm{m}}, \mathbf{s}, \lambda_{\boldsymbol{f}}) - \chi I_{\mathrm{stim}}(t) \\
\partial_t \mathbf{s} &= \mathbf{A}(\varphi_{\mathrm{m}}) \mathbf{s} + \mathbf{b}(\varphi_{\mathrm{m}}) \\
\partial_t [\mathrm{Ca}^{2+}]_{\mathrm{i}} &= \underbrace{}_{\mathcal{E}_1[\varphi_{\mathrm{m}}]} \underbrace{p_1 \varphi_{\mathrm{m}} - p_2 [\mathrm{Ca}^{2+}]_{\mathrm{i}}}_{\mathcal{E}_2[\varphi_{\mathrm{m}}, \boldsymbol{d}, \boldsymbol{s}, [\mathrm{Ca}^{2+}]_{\mathrm{i}}]}
\end{aligned}
$$

➔ Decouples into two PDEs ($\mathcal{M}, \mathcal{E}_1$) and nonlinear, spatially decoupled ODEs ($\mathcal{E}_2$)

Numerical Scheme

Multi-Mesh Method

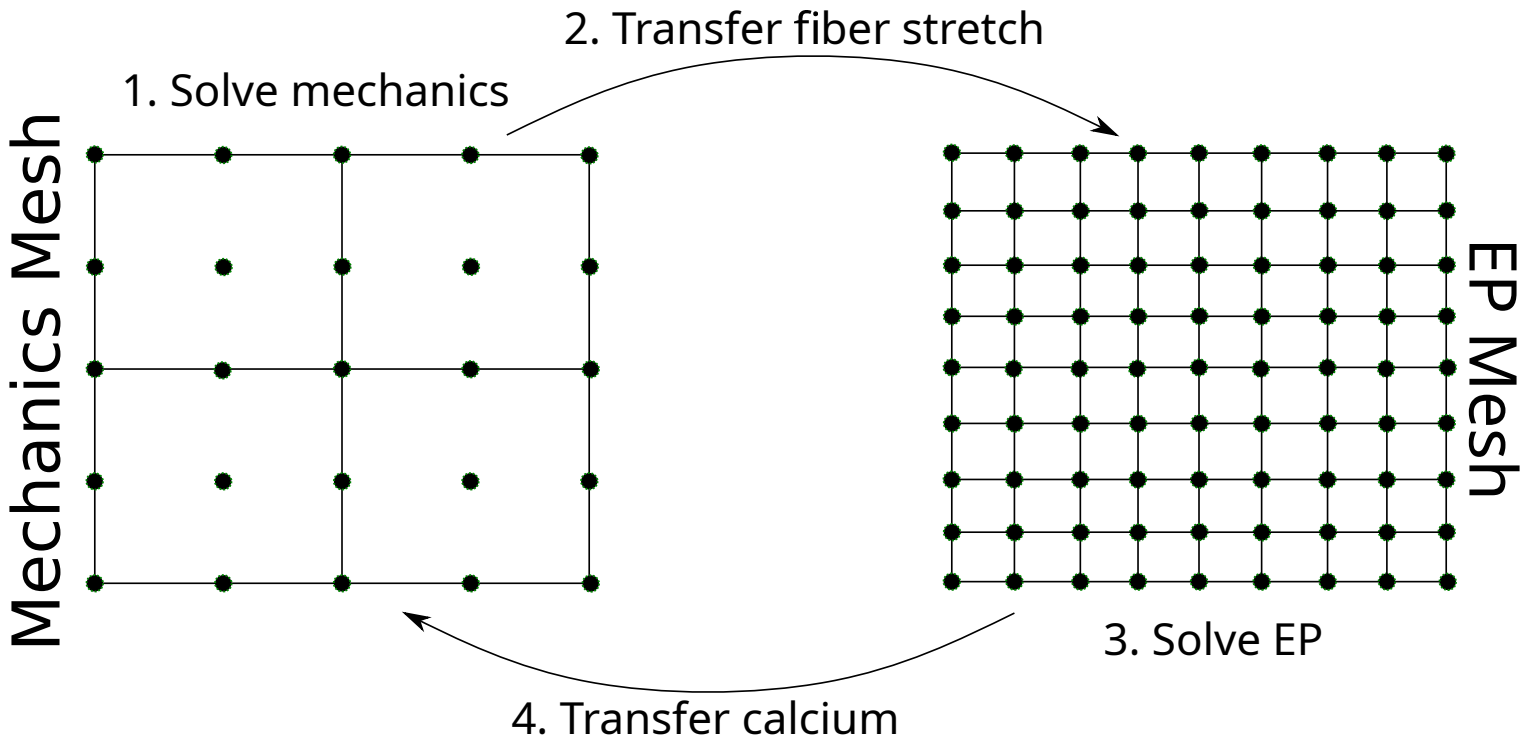

Note on Step 2: Stretch is described by the gradient of $\boldsymbol{d}$!

➔ L_2-projection on mechanics mesh nodes

Note on RTC: We chose $\Delta t_{\max}$ dependent on Δt_{mech} to match the time grid

Modified Niederer Benchmark: Electrical Stimulation

Based on Niederer et al. [2011]

Setup

- Modified PCG2019 model
- Constrain $\boldsymbol{d} = \mathbf{0}$ on marked side
- $200\,\text{mm} \times 70\,\text{mm} \times 30\,\text{mm}$
- Electrical activation in grey block

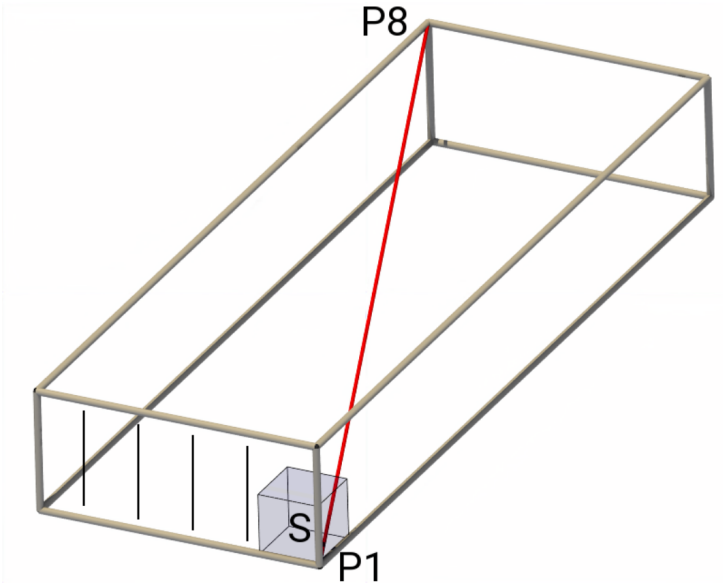

Reference ($\Delta t_{\mathcal{M}}$=0.1 ms)

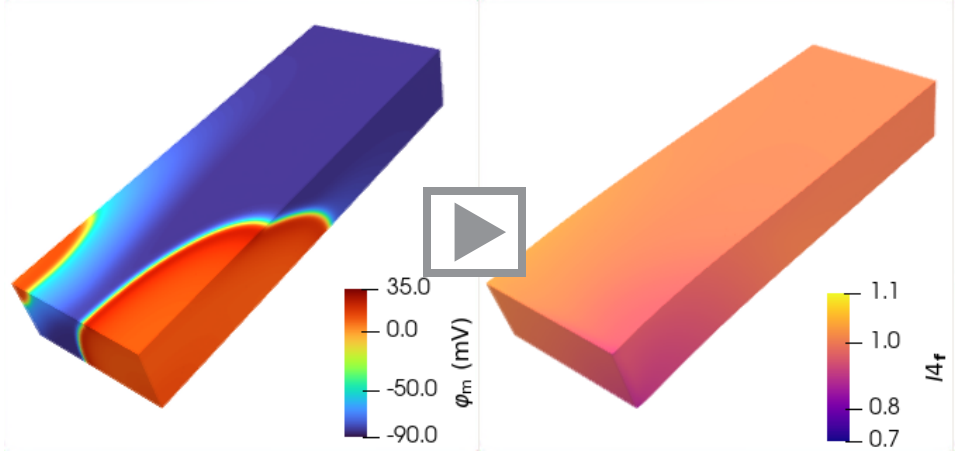

Wallclock time $\approx 7\,\text{h}$

Space-Time Adaptive Method ($\Delta t_{\mathcal{M}}$=0.5 ms)

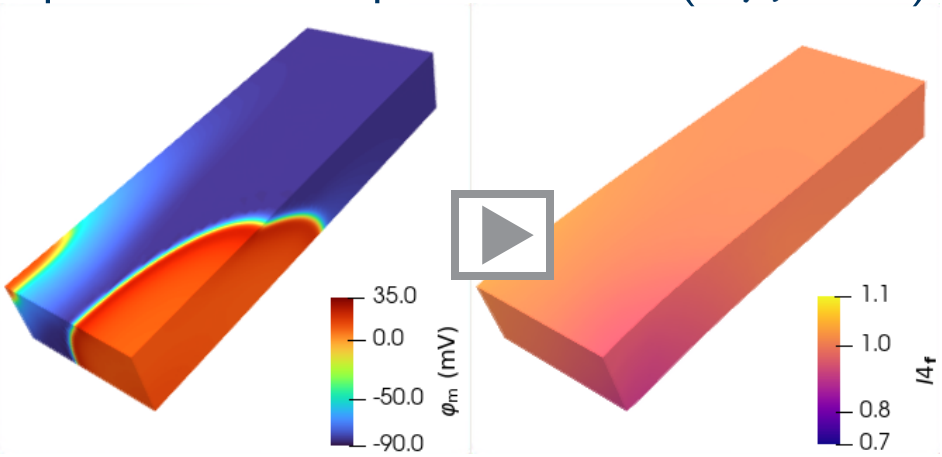

Wallclock time $\approx 2\,\text{min}$

Modified Niederer Benchmark: Electrical Stimulation

Based on Niederer et al. [2011]

Setup

- Modified PCG2019 model
- Constrain $\boldsymbol{d} = \mathbf{0}$ on marked side
- $200\,\text{mm} \times 70\,\text{mm} \times 30\,\text{mm}$
- Electrical activation in grey block

➔ **speedup of $\approx 100\times$**

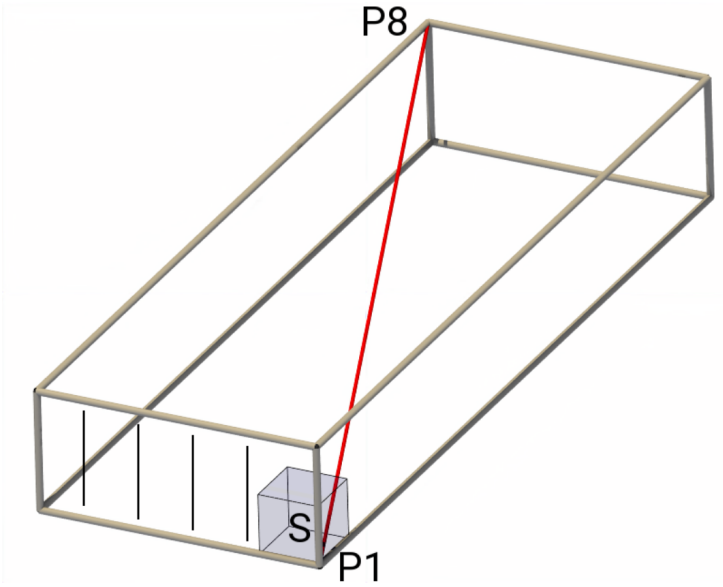

Reference ($\Delta t_{\mathcal{M}}$=0.1 ms)

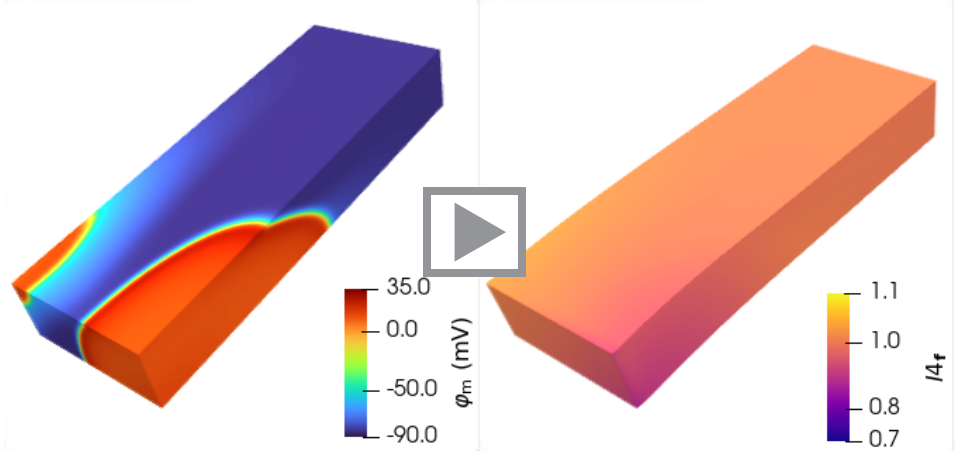

Wallclock time $\approx 7\,\text{h}$

Space-Time Adaptive Method ($\Delta t_{\mathcal{M}}$=0.5 ms)

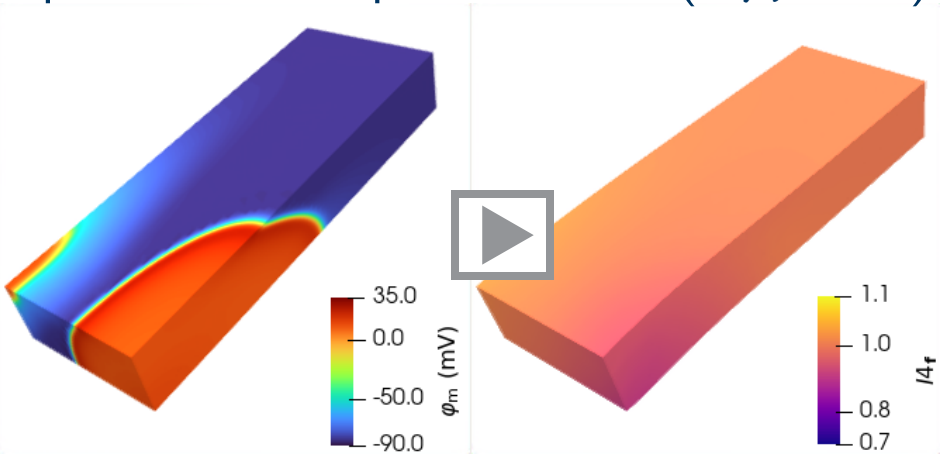

Wallclock time $\approx 2\,\text{min}$

Biventricular Rabbit Model

Derived from Krishnamoorthi et al. [2014].

Setup

- Coarsened mesh
- Project measured microstructure
- Purkinje network for activation
- $d = 0$ for the most apical faces

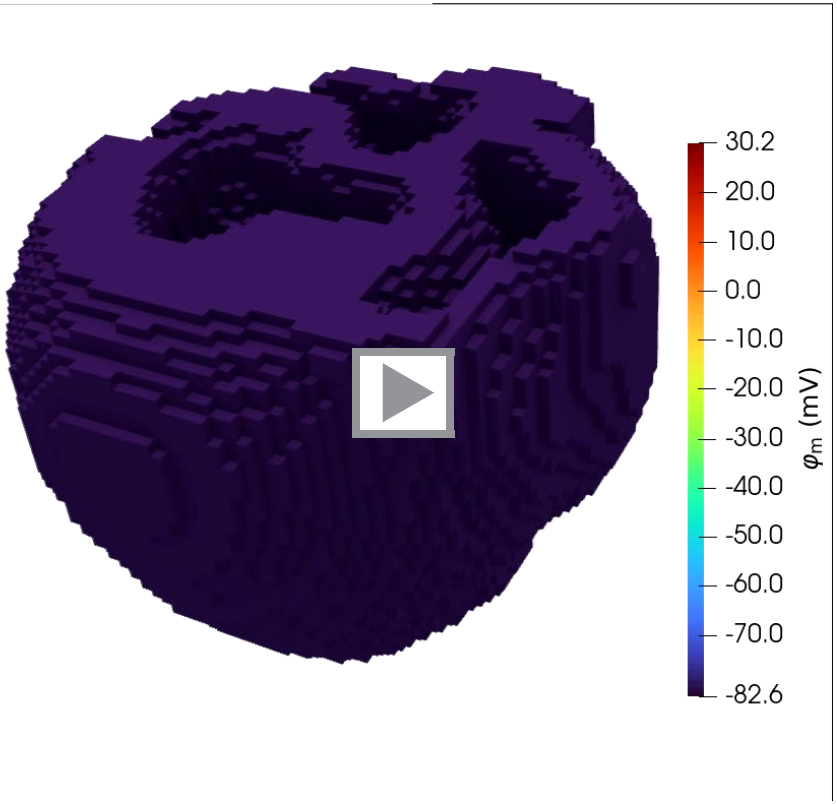

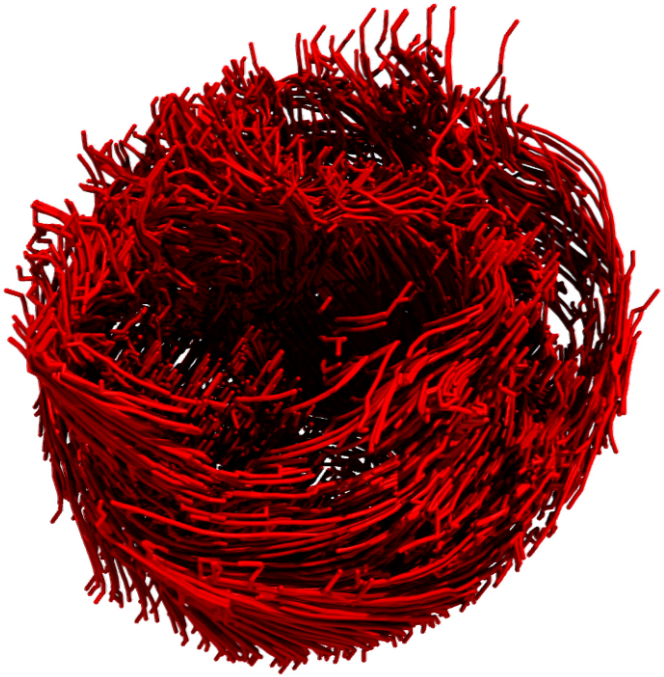

Results

Relevant features are present and qualitatively resolved, e.g.:

- Conduction velocity
- Wall-thickening

→ ≈ 56m wallclock time

Computing Meets Cardiology: Making Heart Simulations Fast and Accurate

Summary

- Hierarchical operator split of electromechanical cardiac model
- AMR of EP via Kelly error indicator
- Time adaptivity of EP via reaction-tangent controller

➔ About **two orders** of magnitude speedup over naive strategies

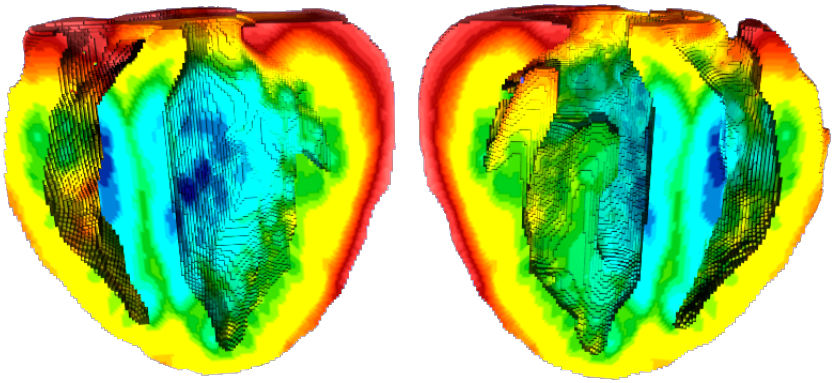

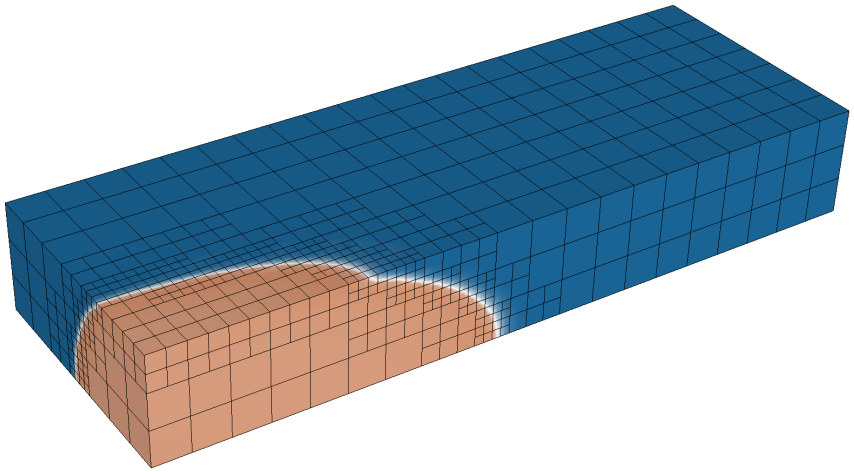

Future Work

- Local adaptive time integration schemes
- Improved cell models with biophysically accurate mechanics interaction
- Validated setup to simulate correct activation and motion robustly

➔ Fast & accurate 4-chamber simulations